

# A General Analysis of $\gamma$ Determinations from $B \rightarrow \pi K$ Decays

Andrzej J. Buras<sup>1,2</sup> and Robert Fleischer<sup>1</sup>

<sup>1</sup>*Theory Division, CERN, CH-1211 Geneva 23, Switzerland*

<sup>2</sup>*Technische Universität München, Physik Department  
D-85748 Garching, Germany*

## Abstract

We present a general parametrization of  $B^\pm \rightarrow \pi^\pm K$ ,  $\pi^0 K^\pm$  and  $B_d \rightarrow \pi^0 K$ ,  $\pi^\mp K^\pm$  decays, taking into account both electroweak penguin and rescattering effects. This formalism allows – among other things – an improved implementation of the strategies that were recently proposed by Neubert and Rosner to probe the CKM angle  $\gamma$  with the help of  $B^\pm \rightarrow \pi^\pm K$ ,  $\pi^0 K^\pm$  decays. In particular, it allows us to investigate the sensitivity of the extracted value of  $\gamma$  to the basic assumptions of their approach. We find that certain  $SU(3)$ -breaking effects may have an important impact and emphasize that additional hadronic uncertainties are due to rescattering processes. The latter can be controlled by using  $SU(3)$  flavour symmetry arguments and additional experimental information provided by  $B^\pm \rightarrow K^\pm K$  modes. We propose a new strategy to probe the angle  $\gamma$  with the help of the neutral decays  $B_d \rightarrow \pi^0 K$ ,  $\pi^\mp K^\pm$ , which is theoretically cleaner than the  $B^\pm \rightarrow \pi^\pm K$ ,  $\pi^0 K^\pm$  approach. Here rescattering processes can be taken into account by just measuring the CP-violating observables of the decay  $B_d \rightarrow \pi^0 K_S$ . Finally, we point out that an experimental analysis of  $B_s \rightarrow K^+ K^-$  modes would also be very useful to probe the CKM angle  $\gamma$ , as well as electroweak penguins, and we critically compare the virtues and weaknesses of the various approaches discussed in this paper. As a by-product, we point out a strategy to include the electroweak penguins in the determination of the CKM angle  $\alpha$  from  $B \rightarrow \pi\pi$  decays.



# 1 Introduction

Last year, the CLEO collaboration reported the observation of several exclusive  $B$ -meson decays into two light pseudoscalar mesons [1], which led to great excitement in the  $B$ -physics community. In particular, the decays  $B^+ \rightarrow \pi^+ K^0$ ,  $B_d^0 \rightarrow \pi^- K^+$  and their charge conjugates received a lot of attention [2], since their observables may provide useful information on the angle  $\gamma$  of the usual non-squashed unitarity triangle of the Cabibbo–Kobayashi–Maskawa matrix (CKM matrix) [3, 4]. So far, only results for the combined branching ratios

$$\text{BR}(B^\pm \rightarrow \pi^\pm K) \equiv \frac{1}{2} [\text{BR}(B^+ \rightarrow \pi^+ K^0) + \text{BR}(B^- \rightarrow \pi^- \overline{K}^0)] \quad (1)$$

$$\text{BR}(B_d \rightarrow \pi^\mp K^\pm) \equiv \frac{1}{2} [\text{BR}(B_d^0 \rightarrow \pi^- K^+) + \text{BR}(\overline{B}_d^0 \rightarrow \pi^+ K^-)] \quad (2)$$

have been published, with values at the  $10^{-5}$  level and large experimental uncertainties. As was pointed out in [5], already these combined branching ratios may lead to highly non-trivial constraints on  $\gamma$ , which become effective if the ratio

$$R \equiv \frac{\text{BR}(B_d \rightarrow \pi^\mp K^\pm)}{\text{BR}(B^\pm \rightarrow \pi^\pm K)} \quad (3)$$

is found to be smaller than 1. If we use the  $SU(2)$  isospin symmetry of strong interactions and neglect certain rescattering and electroweak penguin effects (for more sophisticated strategies, taking into account also these effects, see [6, 7]), we obtain the following allowed range for  $\gamma$  [5]:

$$0^\circ \leq \gamma \leq \gamma_0 \quad \vee \quad 180^\circ - \gamma_0 \leq \gamma \leq 180^\circ, \quad (4)$$

where  $\gamma_0$  is given by

$$\gamma_0 = \arccos(\sqrt{1 - R}). \quad (5)$$

Unfortunately, the present data do not yet provide a definite answer to the question of whether  $R < 1$ . The results reported by the CLEO collaboration last year gave  $R = 0.65 \pm 0.40$  [1], whereas a recent, preliminary update yields  $R = 1.0 \pm 0.4$  [8]. A detailed study of the implications of (4) for the determination of the unitarity triangle was performed in [9].

This summer, the CLEO collaboration announced the first observation of another  $B \rightarrow \pi K$  decay, which is the mode  $B^\pm \rightarrow \pi^0 K^\pm$  [8]. Consequently, it is natural to ask whether we could also obtain interesting information on the angle  $\gamma$  with the help of this decay. In fact, several years ago, Gronau, Rosner and London (GRL) proposed an interesting strategy to determine  $\gamma$ , with the help of the decays  $B^+ \rightarrow \pi^0 K^+$ ,  $B^+ \rightarrow \pi^+ K^0$ ,  $B^+ \rightarrow \pi^+ \pi^0$  and their charge conjugates, by using the  $SU(3)$  flavour symmetry of strong interactions [10] (see also [11]). However, as was pointed out by Deshpande and He [12], this elegant approach is unfortunately spoiled by electroweak penguins, which play

an important role in several non-leptonic  $B$ -meson decays because of the large top-quark mass [13, 14]. In the case of the mode  $B^+ \rightarrow \pi^0 K^+$ , electroweak penguins contribute both in “colour-allowed” and in “colour-suppressed” form, whereas only electroweak penguin topologies of the latter kind contribute to the decays  $B^+ \rightarrow \pi^+ K^0$  and  $B_d^0 \rightarrow \pi^- K^+$ . Performing model calculations within the framework of the “factorization” hypothesis, one finds that “colour-suppressed” electroweak penguins play a negligible role [15]. These crude estimates may, however, underestimate the role of these topologies [4, 16], which therefore represent an important limitation of the theoretical accuracy of the strategies to probe the CKM angle  $\gamma$  with the help of  $B^\pm \rightarrow \pi^\pm K$  and  $B_d \rightarrow \pi^\mp K^\pm$  decays [2].

In [3, 17], we proposed methods to obtain experimental insights into electroweak penguins with the help of amplitude relations between the  $B \rightarrow \pi K$  decays listed above. Since it is possible to derive a transparent expression for the relevant electroweak penguin amplitude by performing appropriate Fierz transformations of the electroweak penguin operators and using the  $SU(3)$  flavour symmetry [3] (see also [14]), the experimental determination of this amplitude would allow an interesting test of the Standard Model. In two recent papers [18, 19], Neubert and Rosner used a more elaborate, but similar theoretical input to calculate the electroweak penguin amplitude affecting the GRL approach. Provided the electroweak penguin amplitude calculated this way is theoretically reliable, the combined  $B^\pm \rightarrow \pi^\pm K$  and  $B^\pm \rightarrow \pi^0 K^\pm$  branching ratios may imply interesting bounds on the CKM angle  $\gamma$  [18], and the original GRL strategy, requiring the measurement of a CP-violating asymmetry in  $B^\pm \rightarrow \pi^0 K^\pm$ , is resurrected [19].

In this paper, we point out that the general formulae to probe the CKM angle  $\gamma$ , with the help of the decays  $B^\pm \rightarrow \pi^\pm K$  and  $B_d \rightarrow \pi^\mp K^\pm$  that were derived in [6], apply also to the combination  $B^\pm \rightarrow \pi^\pm K, \pi^0 K^\pm$  of charged  $B$  decays, as well as to the combination  $B_d \rightarrow \pi^0 K, \pi^\mp K^\pm$  of neutral  $B$  decays, if straightforward replacements of variables are performed. In this manner, the virtues and weaknesses of the strategies proposed in [6, 18, 19], and of a new one proposed here, can be systematically investigated and compared with one another. Following these lines, we are in a position to derive the bounds on  $\gamma$  arising in the  $B^\pm \rightarrow \pi^\pm K, \pi^0 K^\pm$  case [18] in a general and transparent way. In contrast to the expressions given in [18], our formalism is valid *exactly* and does not rely on any expansion in a small parameter. Moreover, it allows us to investigate the sensitivity of the value of  $\gamma$  to the basic assumptions made in [18], and to take into account certain rescattering processes by using the strategies proposed in [6, 7]. These final-state interaction effects were neglected by Neubert and Rosner in [18, 19], but may in principle play an important role [16, 20–24]. We find that they lead to uncertainties similar to those affecting the  $B^\pm \rightarrow \pi^\pm K, B_d \rightarrow \pi^\mp K^\pm$  strategies [2], and that furthermore certain  $SU(3)$ -breaking effects may have an important impact. Concerning rescattering effects, the neutral decays  $B_d \rightarrow \pi^0 K, \pi^\mp K^\pm$  offer theoretically cleaner strategies to probe the CKM angle  $\gamma$  than the charged modes  $B^\pm \rightarrow \pi^\pm K, \pi^0 K^\pm$ . The point is that the decay  $B_d \rightarrow \pi^0 K_S$  provides an additional observable, which originates from mixing-induced CP violation. If we use in addition the CP asymmetry arising in the mode  $B_d \rightarrow J/\psi K_S$  to fix the  $B_d^0\text{--}\overline{B}_d^0$  mixing phase, the rescattering processes can be included completely. We also point out that an experimental analysis of the decay  $B_s \rightarrow K^+ K^-$  would offer

– in combination with the data provided by  $B_d \rightarrow \pi^\mp K^\pm$ ,  $B^\pm \rightarrow \pi^\pm K$  and  $B^\pm \rightarrow \pi^\pm \pi$   
– several simple strategies both to probe the CKM angle  $\gamma$  and to obtain insights into electroweak penguins. Therefore, an accurate measurement of the decay  $B_s \rightarrow K^+ K^-$ , which should be feasible at future hadron machines, would be an important goal.

The outline of this paper is as follows: in Section 2, we present a general parametrization of the  $B \rightarrow \pi K$  decay amplitudes and observables, taking into account both electroweak penguin and rescattering effects. In Section 3, we recapitulate the  $B^\pm \rightarrow \pi^\pm K$ ,  $B_d \rightarrow \pi^\mp K^\pm$  strategies to constrain and determine the CKM angle  $\gamma$  in the light of the most recent CLEO data, and point out some interesting features that were not emphasized in previous work. In Section 4, we focus on strategies to probe  $\gamma$  with the help of the charged decays  $B^\pm \rightarrow \pi^\pm K$ ,  $\pi^0 K^\pm$ , while we turn to a new approach, using the neutral modes  $B_d \rightarrow \pi^0 K$ ,  $\pi^\mp K^\pm$ , in Section 5. Several strategies to combine the observables of the  $B_{u,d} \rightarrow \pi K$  modes with those of the decay  $B_s \rightarrow K^+ K^-$  to determine the CKM angle  $\gamma$  and to probe electroweak penguins are proposed in Section 6. Finally, the conclusions are summarized in Section 7, where we also critically compare the virtues and weaknesses of the various approaches discussed in this paper. In an appendix, we present a by-product of our considerations, allowing us to include electroweak penguin topologies in the determination of the CKM angle  $\alpha$  from  $B \rightarrow \pi\pi$  decays.

## 2 Decay Amplitudes and Observables

In this section, we will closely follow Ref. [6] to parametrize the decay amplitudes and observables of  $B^\pm \rightarrow \pi^0 K^\pm$  and  $B_d \rightarrow \pi^0 K$  arising within the framework of the Standard Model. Before turning to these modes, it will be instructive to recall certain features of the decays  $B^\pm \rightarrow \pi^\pm K$  and  $B_d \rightarrow \pi^\mp K^\pm$ , which were already discussed in detail in [6].

### 2.1 The Decays $B^\pm \rightarrow \pi^\pm K$ and $B_d \rightarrow \pi^\mp K^\pm$

In order to probe the CKM angle  $\gamma$  through these decays, the central role is played by the following amplitude relation:

$$A(B^+ \rightarrow \pi^+ K^0) + A(B_d^0 \rightarrow \pi^- K^+) = -[T + P_{\text{ew}}^{\text{C}}], \quad (6)$$

which can be derived by using the  $SU(2)$  isospin symmetry of strong interactions [25]. Here the amplitude  $T$ , which is usually referred to as a “tree” amplitude, takes the form

$$T = |T| e^{i\delta_T} e^{i\gamma}. \quad (7)$$

Owing to a subtlety in the implementation of the isospin symmetry, the amplitude  $T$  does not only receive contributions from colour-allowed  $\bar{b} \rightarrow \bar{u}u\bar{s}$  tree-diagram-like topologies, but also from penguin and annihilation topologies [6, 25]. On the other hand, the quantity  $P_{\text{ew}}^{\text{C}}$  is due to electroweak penguin contributions, which do not carry the phase  $e^{i\gamma}$ , and can be expressed as

$$P_{\text{ew}}^{\text{C}} = -|P_{\text{ew}}^{\text{C}}| e^{i\delta_{\text{ew}}^{\text{C}}}. \quad (8)$$

Note that the remaining electroweak penguin contributions have been absorbed in the amplitude  $T$ . The label “C” reminds us that only “colour-suppressed” electroweak penguin topologies contribute to  $P_{\text{ew}}^{\text{C}}$ . In (7) and (8),  $\delta_T$  and  $\delta_{\text{ew}}^{\text{C}}$  denote CP-conserving strong phases. Explicit formulae for  $T$  and  $P_{\text{ew}}^{\text{C}}$  are given in [6].

The  $B^+ \rightarrow \pi^+ K^0$  decay amplitude entering (6) can be expressed as follows [6]:

$$A(B^+ \rightarrow \pi^+ K^0) = \lambda_u^{(s)} [P_u + P_{\text{ew}}^{(u)\text{C}} + \mathcal{A}] + \lambda_c^{(s)} [P_c + P_{\text{ew}}^{(c)\text{C}}] + \lambda_t^{(s)} [P_t + P_{\text{ew}}^{(t)\text{C}}], \quad (9)$$

where  $P_q$  and  $P_{\text{ew}}^{(q)\text{C}}$  denote contributions from QCD and electroweak penguin topologies with internal  $q$  quarks ( $q \in \{u, c, t\}$ ), respectively;  $\mathcal{A}$  describes annihilation topologies, and  $\lambda_q^{(s)} \equiv V_{qs} V_{qb}^*$  are the usual CKM factors. If we make use of the unitarity of the CKM matrix and apply the Wolfenstein parametrization [26], generalized to include non-leading terms in  $\lambda$  [27], we obtain [6]

$$A(B^+ \rightarrow \pi^+ K^0) \equiv P = - \left(1 - \frac{\lambda^2}{2}\right) \lambda^2 A [1 + \rho e^{i\theta} e^{i\gamma}] \mathcal{P}_{tc}, \quad (10)$$

where

$$\mathcal{P}_{tc} \equiv |\mathcal{P}_{tc}| e^{i\delta_{tc}} = P_t - P_c + P_{\text{ew}}^{(t)\text{C}} - P_{\text{ew}}^{(c)\text{C}} \quad (11)$$

and

$$\rho e^{i\theta} = \frac{\lambda^2 R_b}{1 - \lambda^2/2} \left[1 - \left(\frac{\mathcal{P}_{uc} + \mathcal{A}}{\mathcal{P}_{tc}}\right)\right]. \quad (12)$$

In these expressions,  $\delta_{tc}$  and  $\theta$  denote CP-conserving strong phases, and  $\mathcal{P}_{uc}$  is defined in analogy to (11). The quantity  $\rho e^{i\theta}$  is a measure of the strength of certain rescattering effects, and the relevant CKM factors are given by (for a recent update of  $R_b$ , see [28]):

$$\lambda \equiv |V_{us}| = 0.22, \quad A \equiv \frac{1}{\lambda^2} |V_{cb}| = 0.81 \pm 0.06, \quad R_b \equiv \frac{1}{\lambda} \left| \frac{V_{ub}}{V_{cb}} \right| = 0.41 \pm 0.07. \quad (13)$$

In the parametrization of the  $B^\pm \rightarrow \pi^\pm K$  and  $B_d \rightarrow \pi^\mp K^\pm$  observables, it turns out to be useful to introduce the quantities

$$r \equiv \frac{|T|}{\sqrt{\langle |P|^2 \rangle}}, \quad \epsilon_{\text{C}} \equiv \frac{|P_{\text{ew}}^{\text{C}}|}{\sqrt{\langle |P|^2 \rangle}}, \quad (14)$$

with

$$\langle |P|^2 \rangle \equiv \frac{1}{2} (|P|^2 + |\overline{P}|^2), \quad (15)$$

as well as the CP-conserving strong phase differences

$$\delta \equiv \delta_T - \delta_{tc}, \quad \Delta_{\text{C}} \equiv \delta_{\text{ew}}^{\text{C}} - \delta_{tc}. \quad (16)$$

The CP-conjugate amplitude  $\overline{P}$  is obtained from (10) by simply reversing the sign of the weak phase  $\gamma$ . A similar comment applies also to all other CP-conjugate decay amplitudes

appearing in this paper. In addition to the ratio  $R$  of combined  $B \rightarrow \pi K$  branching ratios defined by (3), also the “pseudo-asymmetry”

$$A_0 \equiv \frac{\text{BR}(B_d^0 \rightarrow \pi^- K^+) - \text{BR}(\overline{B}_d^0 \rightarrow \pi^+ K^-)}{\text{BR}(B^+ \rightarrow \pi^+ K^0) + \text{BR}(B^- \rightarrow \pi^- \overline{K}^0)} = A_{\text{CP}}(B_d \rightarrow \pi^\mp K^\pm) R \quad (17)$$

plays an important role to probe the CKM angle  $\gamma$ . Explicit expressions for  $R$  and  $A_0$  in terms of the parameters specified above are given in [6].

As we already noted, the electroweak penguins are “colour-suppressed” in the case of the decays  $B^+ \rightarrow \pi^+ K^0$  and  $B_d^0 \rightarrow \pi^- K^+$ . Calculations performed at the perturbative quark level, where the relevant hadronic matrix elements are treated within the “factorization” approach, typically give  $\epsilon_C = \mathcal{O}(1\%)$  [15]. These crude estimates may, however, underestimate the role of these topologies [4, 16]. An improved theoretical description of the electroweak penguins is possible, using the general expressions for the corresponding four-quark operators, appropriate Fierz transformations and the  $SU(2)$  isospin symmetry. Following these lines [6] (see also [3, 14]), we arrive at

$$\left| \frac{P_{\text{ew}}^C}{T} \right| e^{i(\delta_{\text{ew}}^C - \delta_T)} = - \frac{3}{2\lambda^2 R_b} \left[ \frac{C_9(\mu) + C_{10}(\mu)\zeta(\mu)}{C_1'(\mu) + C_2'(\mu)\zeta(\mu)} \right], \quad (18)$$

with

$$\zeta(\mu) = \frac{\langle K^0 \pi^+ | Q_2^u(\mu) | B^+ \rangle + \langle K^+ \pi^- | Q_2^u(\mu) | B_d^0 \rangle}{\langle K^0 \pi^+ | Q_1^u(\mu) | B^+ \rangle + \langle K^+ \pi^- | Q_1^u(\mu) | B_d^0 \rangle} \quad (19)$$

and

$$C_1'(\mu) \equiv C_1(\mu) + \frac{3}{2} C_9(\mu), \quad C_2'(\mu) \equiv C_2(\mu) + \frac{3}{2} C_{10}(\mu). \quad (20)$$

Here  $C_{1,2}(\mu)$  are the Wilson coefficients of the current–current operators

$$\begin{aligned} Q_1^u &= (\bar{u}_\alpha s_\beta)_{\text{V-A}} (\bar{b}_\beta u_\alpha)_{\text{V-A}} \\ Q_2^u &= (\bar{u}_\alpha s_\alpha)_{\text{V-A}} (\bar{b}_\beta u_\beta)_{\text{V-A}}, \end{aligned} \quad (21)$$

and the coefficients  $C_{9,10}(\mu)$  are those of the electroweak penguin operators

$$\begin{aligned} Q_9 &= \frac{3}{2} (\bar{b}_\alpha s_\alpha)_{\text{V-A}} \sum_{q=u,d,c,s,b} e_q (\bar{q}_\beta q_\beta)_{\text{V-A}} \\ Q_{10} &= \frac{3}{2} (\bar{b}_\alpha s_\beta)_{\text{V-A}} \sum_{q=u,d,c,s,b} e_q (\bar{q}_\beta q_\alpha)_{\text{V-A}}. \end{aligned} \quad (22)$$

As usual,  $\alpha$  and  $\beta$  are colour indices, and  $e_q$  denotes the quark charges. It should be kept in mind that two electroweak penguin operators,  $Q_7$  and  $Q_8$ , with tiny Wilson coefficients, and electroweak penguins with internal charm- and up-quark exchanges were neglected in the derivation of (18). In our numerical estimates given below, it will suffice to use the leading-order values [29]

$$C_1(m_b) = -0.308, \quad C_2(m_b) = 1.144, \quad C_9(m_b)/\alpha = -1.280, \quad C_{10}(m_b)/\alpha = 0.328 \quad (23)$$

with  $\alpha = 1/129$ . It is possible to rewrite (18) as follows [6]:

$$\begin{aligned} \frac{\epsilon_C}{r} e^{i(\Delta_C - \delta)} &= \frac{3}{2\lambda^2 R_b} \left[ \frac{C'_1(\mu)C_9(\mu) - C'_2(\mu)C_{10}(\mu)}{C_2'^2(\mu) - C_1'^2(\mu)} \right. \\ &\quad \left. + a_C e^{i\omega_C} \left\{ \frac{C'_1(\mu)C_{10}(\mu) - C'_2(\mu)C_9(\mu)}{C_2'^2(\mu) - C_1'^2(\mu)} \right\} \right], \end{aligned} \quad (24)$$

where we will neglect the first, strongly suppressed term

$$\frac{C'_1(\mu)C_9(\mu) - C'_2(\mu)C_{10}(\mu)}{C'_1(\mu)C_{10}(\mu) - C'_2(\mu)C_9(\mu)} = \mathcal{O}(10^{-2}) \quad (25)$$

in the following considerations:

$$\frac{\epsilon_C}{r} e^{i(\Delta_C - \delta)} \approx \frac{3}{2\lambda^2 R_b} \left[ \frac{C'_1(\mu)C_{10}(\mu) - C'_2(\mu)C_9(\mu)}{C_2'^2(\mu) - C_1'^2(\mu)} \right] a_C e^{i\omega_C}. \quad (26)$$

The combination of Wilson coefficients in this expression is essentially renormalization-scale-independent and changes only by  $\mathcal{O}(1\%)$  when evolving from  $\mu = M_W$  down to  $\mu = m_b$ . Employing  $R_b = 0.41$  and the Wilson coefficients given in (23) yields [6]

$$\frac{\epsilon_C}{r} e^{i(\Delta_C - \delta)} \approx 0.66 \times a_C e^{i\omega_C}. \quad (27)$$

The quantity  $a_C e^{i\omega_C}$  is given by

$$a_C e^{i\omega_C} \equiv \frac{a_2^{\text{eff}}}{a_1^{\text{eff}}} = \frac{C'_1(\mu)\zeta(\mu) + C'_2(\mu)}{C'_1(\mu) + C'_2(\mu)\zeta(\mu)}, \quad (28)$$

where  $a_1^{\text{eff}}$  and  $a_2^{\text{eff}}$  correspond to a generalization of the usual phenomenological “colour” factors  $a_1$  and  $a_2$ , describing the intrinsic strength of “colour-suppressed” and “colour-allowed” decay processes, respectively [6]. Note that the “factorization” approach gives  $\zeta(\mu_F) = 3$ , where  $\mu_F$  is the “factorization scale”. Comparing experimental data on  $B^- \rightarrow D^{(*)0}\pi^-$  and  $\overline{B}_d^0 \rightarrow D^{(*)+}\pi^-$ , as well as on  $B^- \rightarrow D^{(*)0}\rho^-$  and  $\overline{B}_d^0 \rightarrow D^{(*)+}\rho^-$  decays gives  $a_2/a_1 = \mathcal{O}(0.25)$ . Here  $a_1$  and  $a_2$  are – in contrast to  $a_1^{\text{eff}}$  and  $a_2^{\text{eff}}$  – real quantities, and their relative sign is found to be positive. Experimental studies of  $B \rightarrow J/\psi K^{(*)}$  decays favour also  $|a_2/a_1| = \mathcal{O}(0.25)$ . If we assume that the strength of “colour suppression” in  $B \rightarrow \pi K$  decays is of the same order of magnitude, i.e.  $a_C = 0.25$ , we obtain a value of  $\epsilon_C/r$  that is larger by a factor of 3 than the “factorized” result

$$\left. \frac{\epsilon_C}{r} e^{i(\Delta_C - \delta)} \right|_{\text{fact}} = 0.06 \times \left[ \frac{0.41}{R_b} \right], \quad (29)$$

corresponding to  $\mu = \mu_F$  and  $\zeta(\mu_F) = 3$  in (18). The expression (26) shows nicely that the usual terminology of “colour-suppressed” electroweak penguins in (6) is justified,



since  $P_{\text{ew}}^{\text{C}}$  is proportional to the generalized “colour” factor  $a_2^{\text{eff}}$ . Moreover, it implies a correlation between  $\epsilon_{\text{C}}$  and  $r$ , which is given by

$$\epsilon_{\text{C}} = q_{\text{C}} r, \quad \Delta_{\text{C}} = \delta + \omega_{\text{C}} \quad (30)$$

with

$$q_{\text{C}} \approx 0.66 \times \left[ \frac{0.41}{R_b} \right] \times a_{\text{C}}. \quad (31)$$

The ratio  $R$  defined by (3) can be expressed as follows [6]:

$$R = 1 - \frac{2r}{u} (h \cos \delta + k \sin \delta) + v^2 r^2, \quad (32)$$

where

$$h = \cos \gamma + \rho \cos \theta - q_{\text{C}} [\cos \omega_{\text{C}} + \rho \cos(\theta - \omega_{\text{C}}) \cos \gamma] \quad (33)$$

$$k = \rho \sin \theta + q_{\text{C}} [\sin \omega_{\text{C}} - \rho \sin(\theta - \omega_{\text{C}}) \cos \gamma] \quad (34)$$

and

$$u = \sqrt{1 + 2\rho \cos \theta \cos \gamma + \rho^2} \quad (35)$$

$$v = \sqrt{1 - 2q_{\text{C}} \cos \omega_{\text{C}} \cos \gamma + q_{\text{C}}^2}. \quad (36)$$

The pseudo-asymmetry  $A_0$  (see (17)) takes the form

$$A_0 = A_+ + 2 \frac{r}{u} [\sin \delta + q_{\text{C}} \rho \sin(\delta - \theta + \omega_{\text{C}})] \sin \gamma - 2 q_{\text{C}} r^2 \sin \omega_{\text{C}} \sin \gamma, \quad (37)$$

where

$$A_+ \equiv \frac{\text{BR}(B^+ \rightarrow \pi^+ K^0) - \text{BR}(B^- \rightarrow \pi^- \bar{K}^0)}{\text{BR}(B^+ \rightarrow \pi^+ K^0) + \text{BR}(B^- \rightarrow \pi^- \bar{K}^0)} = - \frac{2\rho \sin \theta \sin \gamma}{1 + 2\rho \cos \theta \cos \gamma + \rho^2} \quad (38)$$

measures direct CP violation in the decay  $B^+ \rightarrow \pi^+ K^0$ . Note that tiny phase-space effects have been neglected in (32) and (37) (for a more detailed discussion, see [5]).

## 2.2 The Decays $B^{\pm} \rightarrow \pi^0 K^{\pm}$ and $B_d \rightarrow \pi^0 K$

Let us now turn to the decays  $B^+ \rightarrow \pi^0 K^+$ ,  $B_d^0 \rightarrow \pi^0 K^0$  and their charge conjugates. The  $SU(2)$  isospin symmetry implies the following amplitude relation [30, 31]:

$$\begin{aligned} A(B^+ \rightarrow \pi^+ K^0) + \sqrt{2} A(B^+ \rightarrow \pi^0 K^+) &= \sqrt{2} A(B_d^0 \rightarrow \pi^0 K^0) + A(B_d^0 \rightarrow \pi^- K^+) \\ &= -[(T + C) + P_{\text{ew}}] \equiv 3 A_{3/2}, \end{aligned} \quad (39)$$

where  $P_{\text{ew}}$  is due to electroweak penguins and  $A_{3/2}$  refers to a  $\pi K$  isospin configuration with  $I = 3/2$ . Note that there is no  $I = 1/2$  component present in (39). Since we have

$$T + C = |T + C| e^{i\delta_{T+C}} e^{i\gamma} \quad (40)$$

and

$$P_{\text{ew}} = -|P_{\text{ew}}|e^{i\delta_{\text{ew}}}, \quad (41)$$

the phase structure of the amplitude relation (39) is completely analogous to the one given in (6). We just have to perform the replacements

$$T \rightarrow T + C \quad \text{and} \quad P_{\text{ew}}^C \rightarrow P_{\text{ew}}. \quad (42)$$

The notation of  $T + C$  reminds us that this amplitude receives contributions both from “colour-allowed” and from “colour-suppressed”  $\bar{b} \rightarrow \bar{u}u\bar{s}$  tree-diagram-like topologies [10]. A similar comment applies to the electroweak penguin amplitude  $P_{\text{ew}}$ , receiving also contributions both from “colour-allowed” and from “colour-suppressed” electroweak penguin topologies [31]. If we neglect electroweak penguin topologies with internal charm and up quarks, as well as the electroweak penguin operators  $Q_7$  and  $Q_8$ , which have tiny Wilson coefficients, perform appropriate Fierz transformations of the remaining electroweak penguin operators  $Q_9$  and  $Q_{10}$  and, moreover, apply the  $SU(2)$  isospin symmetry, we arrive at

$$\left| \frac{P_{\text{ew}}}{T + C} \right| e^{i(\delta_{\text{ew}} - \delta_{T+C})} = -\frac{3}{2\lambda^2 R_b} \left[ \frac{C_9(\mu) + C_{10}(\mu)\tilde{\zeta}(\mu)}{C'_1(\mu) + C'_2(\mu)\tilde{\zeta}(\mu)} \right], \quad (43)$$

with

$$\begin{aligned} \tilde{\zeta}(\mu) &= \frac{\langle K^0 \pi^+ | Q_2^u(\mu) | B^+ \rangle + \sqrt{2} \langle K^+ \pi^0 | Q_2^u(\mu) | B^+ \rangle}{\langle K^0 \pi^+ | Q_1^u(\mu) | B^+ \rangle + \sqrt{2} \langle K^+ \pi^0 | Q_1^u(\mu) | B^+ \rangle} \\ &= \frac{\sqrt{2} \langle K^0 \pi^0 | Q_2^u(\mu) | B_d^0 \rangle + \langle K^+ \pi^- | Q_2^u(\mu) | B_d^0 \rangle}{\sqrt{2} \langle K^0 \pi^0 | Q_1^u(\mu) | B_d^0 \rangle + \langle K^+ \pi^- | Q_1^u(\mu) | B_d^0 \rangle} \equiv \frac{\langle Q_2^u(\mu) \rangle}{\langle Q_1^u(\mu) \rangle}, \end{aligned} \quad (44)$$

which is completely analogous to (18) and (19). Since the  $SU(3)$  flavour symmetry of strong interactions implies

$$\langle Q_1^u(\mu) \rangle = \langle Q_2^u(\mu) \rangle, \quad (45)$$

it is useful to rewrite (43) as follows:

$$\left| \frac{P_{\text{ew}}}{T + C} \right| e^{i(\delta_{\text{ew}} - \delta_{T+C})} = -\frac{3}{2\lambda^2 R_b} \left[ \frac{C_9(\mu) + C_{10}(\mu) + \{C_9(\mu) - C_{10}(\mu)\} \zeta_{SU(3)}(\mu)}{C'_1(\mu) + C'_2(\mu) + \{C'_1(\mu) - C'_2(\mu)\} \zeta_{SU(3)}(\mu)} \right], \quad (46)$$

where

$$\begin{aligned} \zeta_{SU(3)}(\mu) &= \frac{1 - \tilde{\zeta}(\mu)}{1 + \tilde{\zeta}(\mu)} = \frac{\langle K^0 \pi^+ | [Q_1^u(\mu) - Q_2^u(\mu)] | B^+ \rangle + \sqrt{2} \langle K^+ \pi^0 | [Q_1^u(\mu) - Q_2^u(\mu)] | B^+ \rangle}{\langle K^0 \pi^+ | [Q_1^u(\mu) + Q_2^u(\mu)] | B^+ \rangle + \sqrt{2} \langle K^+ \pi^0 | [Q_1^u(\mu) + Q_2^u(\mu)] | B^+ \rangle} \\ &= \frac{\sqrt{2} \langle K^0 \pi^0 | [Q_1^u(\mu) - Q_2^u(\mu)] | B_d^0 \rangle + \langle K^+ \pi^- | [Q_1^u(\mu) - Q_2^u(\mu)] | B_d^0 \rangle}{\sqrt{2} \langle K^0 \pi^0 | [Q_1^u(\mu) + Q_2^u(\mu)] | B_d^0 \rangle + \langle K^+ \pi^- | [Q_1^u(\mu) + Q_2^u(\mu)] | B_d^0 \rangle} \end{aligned} \quad (47)$$

describes  $SU(3)$ -breaking corrections. In the strict  $SU(3)$  limit, we have  $\zeta_{SU(3)}(\mu) = 0$ , and obtain [18]

$$\begin{aligned} \left| \frac{P_{\text{ew}}}{T+C} \right| e^{i(\delta_{\text{ew}} - \delta_{T+C})} &\equiv q e^{i\omega} \approx -\frac{3}{2\lambda^2 R_b} \left[ \frac{C_9(\mu) + C_{10}(\mu)}{C'_1(\mu) + C'_2(\mu)} \right] \\ &\approx \frac{3}{2\lambda^2 R_b} \left[ \frac{C'_1(\mu)C_{10}(\mu) - C'_2(\mu)C_9(\mu)}{C'^2_2(\mu) - C'^2_1(\mu)} \right] = 0.66 \times \left[ \frac{0.41}{R_b} \right], \end{aligned} \quad (48)$$

which is related to  $q_C e^{i\omega_C}$  through

$$q_C e^{i\omega_C} \approx q e^{i\omega} \times a_C. \quad (49)$$

Here we have again neglected the strongly suppressed term (25). Within the “factorization” approximation, we have very small  $SU(3)$ -breaking corrections at the level of a few per cent [18] (see also [3]). Unfortunately, we have no insights into non-factorizable  $SU(3)$  breaking at present. Taking into account both the factorizable corrections, which shift  $q$  from 0.66 to 0.63, and the present experimental uncertainty of  $R_b$  (see (13)), Neubert and Rosner give the range of  $q = 0.63 \pm 0.15$  [18].

If we compare (39) with (6), we find that the observables of the charged  $B$ -meson decays  $B^\pm \rightarrow \pi^\pm K$ ,  $\pi^0 K^\pm$  corresponding to  $R$  and  $A_0$  have to be defined as follows:

$$R_c \equiv 2 \left[ \frac{\text{BR}(B^+ \rightarrow \pi^0 K^+) + \text{BR}(B^- \rightarrow \pi^0 K^-)}{\text{BR}(B^+ \rightarrow \pi^+ K^0) + \text{BR}(B^- \rightarrow \pi^- \bar{K}^0)} \right] \quad (50)$$

$$A_0^c \equiv 2 \left[ \frac{\text{BR}(B^+ \rightarrow \pi^0 K^+) - \text{BR}(B^- \rightarrow \pi^0 K^-)}{\text{BR}(B^+ \rightarrow \pi^+ K^0) + \text{BR}(B^- \rightarrow \pi^- \bar{K}^0)} \right] = A_{\text{CP}}(B^\pm \rightarrow \pi^0 K^\pm) R_c. \quad (51)$$

Concerning strategies to probe the CKM angle  $\gamma$ , the ratio  $R_c$  is more convenient than the quantity  $R_* = 1/R_c$ , which was considered by Neubert and Rosner in [18]. The preliminary results on the CP-averaged branching ratios

$$\text{BR}(B^\pm \rightarrow \pi^0 K^\pm) = (1.5 \pm 0.4 \pm 0.3) \times 10^{-5} \quad (52)$$

$$\text{BR}(B^\pm \rightarrow \pi^\pm K) = (1.4 \pm 0.5 \pm 0.2) \times 10^{-5}, \quad (53)$$

which, very recently, were reported by the CLEO collaboration [8], give

$$R_c = 2.1 \pm 1.1. \quad (54)$$

Here we have added the errors in quadrature. This result differs significantly from the present value of  $R = 1.0 \pm 0.4$ , although the uncertainties are too large to say anything definite.

In the case of the neutral modes  $B_d \rightarrow \pi^0 K$ ,  $\pi^\mp K^\pm$ , we have

$$R_n \equiv \frac{1}{2} \left[ \frac{\text{BR}(B_d^0 \rightarrow \pi^- K^+) + \text{BR}(\bar{B}_d^0 \rightarrow \pi^+ K^-)}{\text{BR}(B_d^0 \rightarrow \pi^0 K^0) + \text{BR}(\bar{B}_d^0 \rightarrow \pi^0 \bar{K}^0)} \right] \quad (55)$$

$$A_0^n \equiv \frac{1}{2} \left[ \frac{\text{BR}(B_d^0 \rightarrow \pi^- K^+) - \text{BR}(\bar{B}_d^0 \rightarrow \pi^+ K^-)}{\text{BR}(B_d^0 \rightarrow \pi^0 K^0) + \text{BR}(\bar{B}_d^0 \rightarrow \pi^0 \bar{K}^0)} \right] = A_{\text{CP}}(B_d \rightarrow \pi^\mp K^\pm) R_n. \quad (56)$$

While the CLEO collaboration recently reported the preliminary result [8]

$$\text{BR}(B_d \rightarrow \pi^\mp K^\pm) = (1.4 \pm 0.3 \pm 0.2) \times 10^{-5}, \quad (57)$$

there is at present only an upper limit available for the decay  $B_d \rightarrow \pi^0 K$ , which is given by  $\text{BR}(B_d \rightarrow \pi^0 K) < 4.1 \times 10^{-5}$  [1].

The parametrization of the observables  $R_c$ ,  $A_0^c$  and  $R_n$ ,  $A_0^n$  is completely analogous to (32) and (37) and can be obtained straightforwardly from these expressions by performing appropriate replacements. The most obvious one is the following:

$$q_C e^{i\omega_C} \rightarrow q e^{i\omega}. \quad (58)$$

Moreover, we have to substitute

$$r \rightarrow r_c \equiv \frac{|T+C|}{\sqrt{\langle |P|^2 \rangle}}, \quad \delta \rightarrow \delta_c \equiv \delta_{T+C} - \delta_{tc} \quad (59)$$

in the case of the observables  $R_c$  and  $A_0^c$ . The parameter  $\rho e^{i\theta}$ , which is defined through the  $B^+ \rightarrow \pi^+ K^0$  decay amplitude, remains unchanged. This is in contrast to the case of the neutral modes  $B_d \rightarrow \pi^0 K$ ,  $\pi^\mp K^\pm$ . Here the decay  $B_d^0 \rightarrow \pi^0 K^0$  takes the role of the mode  $B^+ \rightarrow \pi^+ K^0$ . In analogy to (10), its decay amplitude can be expressed as

$$\sqrt{2} A(B_d^0 \rightarrow \pi^0 K^0) \equiv P_n = - \left( 1 - \frac{\lambda^2}{2} \right) \lambda^2 A \left[ 1 + \rho_n e^{i\theta_n} e^{i\gamma} \right] \mathcal{P}_{tc}^n, \quad (60)$$

where  $\rho_n e^{i\theta_n}$  takes the form

$$\rho_n e^{i\theta_n} = \frac{\lambda^2 R_b}{1 - \lambda^2/2} \left[ 1 - \left( \frac{\mathcal{P}_{uc}^n - \mathcal{C}}{\mathcal{P}_{tc}^n} \right) \right]. \quad (61)$$

Here  $\mathcal{P}_{tc}^n \equiv |\mathcal{P}_{tc}^n| e^{i\delta_{tc}^n}$  and  $\mathcal{P}_{uc}^n$  correspond to differences of penguin topologies with internal top and charm and up and charm quarks, respectively (see (11)). In contrast to the  $B^+ \rightarrow \pi^+ K^0$  case, these quantities receive contributions also from “colour-allowed” electroweak penguin topologies. The amplitude  $\mathcal{C}$  is due to insertions of the current–current operators (21) into “colour-suppressed” tree-diagram-like topologies. In order to parametrize the observables  $R_n$  and  $A_0^n$  with the help of (32) and (37), we have – in addition to (58) – to perform the following replacements:

$$r \rightarrow r_n \equiv \frac{|T+C|}{\sqrt{\langle |P_n|^2 \rangle}}, \quad \delta \rightarrow \delta_n \equiv \delta_{T+C} - \delta_{tc}^n, \quad \rho e^{i\theta} \rightarrow \rho_n e^{i\theta_n}. \quad (62)$$

### 3 Probing the CKM Angle $\gamma$ with the Decays

$$B^\pm \rightarrow \pi^\pm K \text{ and } B_d \rightarrow \pi^\mp K^\pm$$

Before we turn to strategies to constrain and determine the CKM angle  $\gamma$  with the help of the charged decays  $B^\pm \rightarrow \pi^\pm K$ ,  $\pi^0 K^\pm$  in Section 4, and to a new approach dealing with the neutral modes  $B_d \rightarrow \pi^0 K$ ,  $\pi^\mp K^\pm$  in Section 5, let us recapitulate in this section the methods using the decays  $B^\pm \rightarrow \pi^\pm K$  and  $B_d \rightarrow \pi^\mp K^\pm$ . This will allow us, later, to better compare the virtues and weaknesses of all three approaches. Moreover, it is useful to reanalyse the  $B^\pm \rightarrow \pi^\pm K$  and  $B_d \rightarrow \pi^\mp K^\pm$  modes in the light of the most recent CLEO results [8], thereby pointing out some interesting features that had not been emphasized in previous work [2].

#### 3.1 Strategies to Constrain the CKM Angle $\gamma$

Before turning to strategies to extract  $\gamma$ , let us first focus on methods to constrain this angle through the ratio  $R$  of the combined  $B_d \rightarrow \pi^\mp K^\pm$  and  $B^\pm \rightarrow \pi^\pm K$  branching ratios introduced in (3), i.e. without making use of the expected sizeable CP asymmetry arising in  $B_d \rightarrow \pi^\mp K^\pm$ . At present, CP-violating effects in  $B \rightarrow \pi K$  decays have not yet been observed, and only data for the corresponding combined, i.e. CP-averaged, branching ratios are available.

In order to constrain the CKM angle  $\gamma$  with the help of the observable  $R$ , we keep the CP-conserving strong phase  $\delta$ , which is under no theoretical control and completely unknown at present, as a free parameter [5]. Using the general expression (32), we find that  $R$  takes the following extremal values:

$$R_{\min}^{\max}|_\delta = 1 \pm 2 \frac{r}{u} \sqrt{h^2 + k^2} + v^2 r^2, \quad (63)$$

which constrain  $\gamma$ , provided  $r$  can be determined (in [5], a different approach was used to derive these constraints for the special case of neglected rescattering and electroweak penguin effects, i.e. for  $\rho = q_C = 0$ ). In the case of the decays  $B^\pm \rightarrow \pi^\pm K$  and  $B_d \rightarrow \pi^\mp K^\pm$ , flavour symmetry arguments are not sufficient to fix the parameter  $r$  – this is in contrast to the case of  $r_{c,n}$  of the “charged” and “neutral” strategies discussed in the following sections – and an additional input, for example “factorization” or the neglect of “colour-suppressed” topologies in the decay  $B^+ \rightarrow \pi^+ \pi^0$ , have to be used to accomplish this task. Following these lines, present data give  $r = 0.15 \pm 0.05$  [32]. Since the properly defined amplitude  $T$ , which governs the parameter  $r$ , is not just a “tree” amplitude, but receives contributions also from certain penguin and annihilation topologies [6, 25], it is at present difficult to estimate the theoretical uncertainty of  $r$  in a realistic way. Optimistic analyses come to the conclusion that a future theoretical uncertainty of  $\Delta r = \mathcal{O}(10\%)$  may be achievable [4, 33]. However, if rescattering processes of the kind  $B^+ \rightarrow \{\pi^0 K^+\} \rightarrow \pi^+ K^0$  should play an important role, the uncertainties may be significantly larger. Consequently, it would be favourable to have constraints on  $\gamma$  that do not depend on  $r$ .

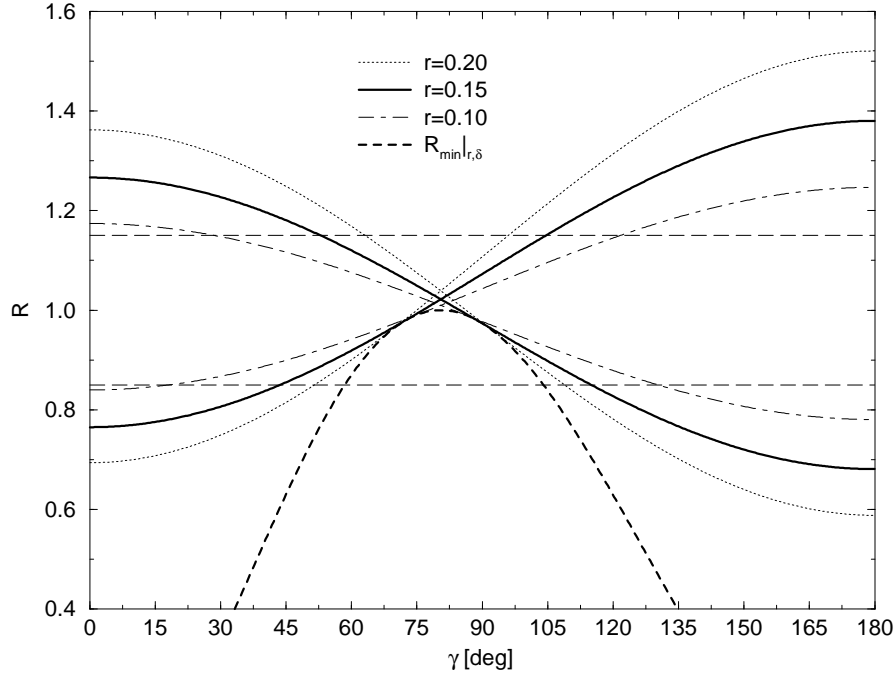


Figure 1: The dependence of the extremal values of  $R$  given in (63) and (64) on the CKM angle  $\gamma$  for  $q_C e^{i\omega_C} = 0.66 \times 0.25$  in the case of negligible rescattering effects, i.e.  $\rho = 0$ .

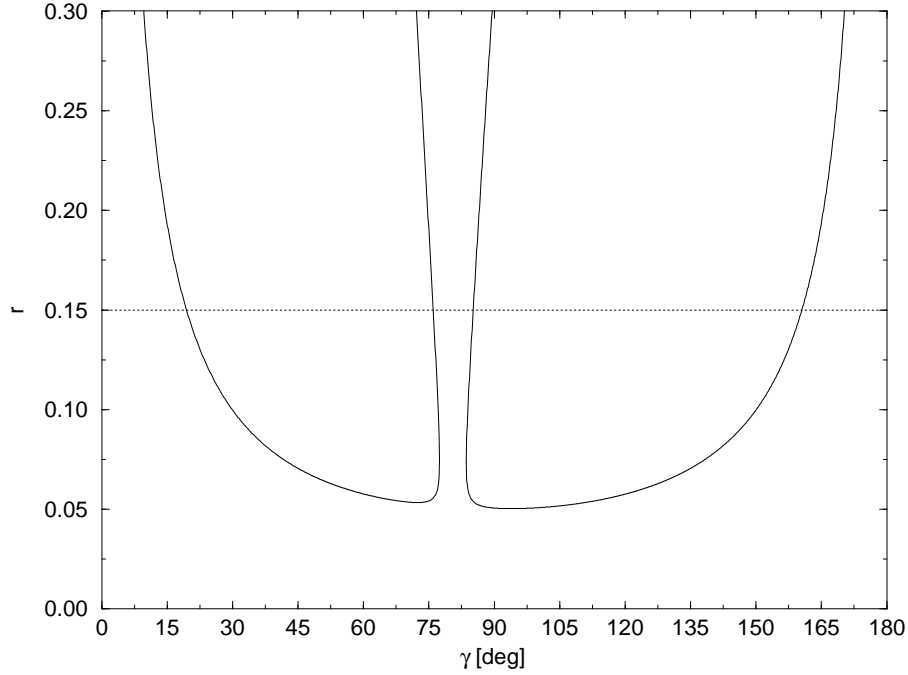


Figure 2: The contours in the  $\gamma$ - $r$  plane corresponding to  $R = 1.00$ ,  $A_0 = 9.96\%$  and  $q_C e^{i\omega_C} = 0.66 \times 0.25$  in the case of negligible rescattering effects, i.e.  $\rho = 0$ .

It was pointed out in [5] that such bounds can be obtained, provided  $R$  is found to be smaller than 1. Within our formalism, they can be derived by keeping both  $\delta$  and  $r$  as free parameters in the general expression (32) for  $R$ . Following these lines, we find that  $R$  takes the minimal value [6]

$$R_{\min}|_{r,\delta} = \left[ \frac{1 + 2 q_C \rho \cos(\theta + \omega_C) + q_C^2 \rho^2}{(1 - 2 q_C \cos \omega_C \cos \gamma + q_C^2)(1 + 2 \rho \cos \theta \cos \gamma + \rho^2)} \right] \sin^2 \gamma, \quad (64)$$

which corresponds to a generalization of the result derived in [5] (see (4) and (5)), and would exclude a certain range of  $\gamma$  around  $90^\circ$ , if  $R$  is found to be smaller than 1. This feature led to great excitement in the  $B$ -physics community, since the first results reported by the CLEO collaboration gave  $R = 0.65 \pm 0.40$  [1]. Unfortunately, a recent, preliminary update yields  $R = 1.0 \pm 0.4$  and is therefore not as promising [8], although it is too early to draw definite conclusions.

In Fig. 1, we have chosen  $q_C e^{i\omega_C} = 0.66 \times 0.25$  and  $\rho = 0$  in order to illustrate the dependence of (63) and (64) on the CKM angle  $\gamma$ . For  $R = 0.85$ , the latter expression would exclude the range of  $58^\circ \leq \gamma \leq 104^\circ$ . The values of  $r$  used to evaluate (63) correspond to the presently allowed range given by Gronau and Rosner [32]. In the future, the corresponding uncertainty of 33% may be reduced by a factor of  $\mathcal{O}(3)$ , provided rescattering processes play a negligible role. On the other hand,  $r$  may in principle be shifted significantly, if rescattering effects should turn out to be large. Important indicators for this unfortunate case would be large direct CP violation in  $B^\pm \rightarrow \pi^\pm K$  modes, and the size of the branching ratios of the decays  $B^\pm \rightarrow K^\pm K$  and  $B_d \rightarrow K^+ K^-$  [6, 7, 24]. In order to illustrate the constraints on  $\gamma$  in more detail, let us assume that  $B^\pm \rightarrow K^\pm K$  and  $B_d \rightarrow K^+ K^-$  indicate that rescattering effects play a very minor role and that the strategies to fix  $r$  (see, for example, [4, 32, 33]) yield  $r = 0.15$ . As can be read off from Fig. 1, the minimal value of  $R$  given in (63) would exclude the range of  $44^\circ \leq \gamma \leq 115^\circ$  in the case of  $R = 0.85$ . If we assume that  $R$  is found to be equal to 1.15, (64) would not be effective. However, the maximal value of  $R$  given in (63) would exclude the range of  $53^\circ \leq \gamma \leq 105^\circ$ .

### 3.2 Strategies to Determine the CKM Angle $\gamma$

As soon as CP violation in  $B_d \rightarrow \pi^\mp K^\pm$  decays is observed, it is possible to go beyond the bounds on  $\gamma$  discussed in the previous subsection. Then we are in a position to eliminate the strong phase  $\delta$  in  $R$  with the help of the pseudo-asymmetry  $A_0$ , thereby fixing contours in the  $\gamma$ - $r$  plane, which are a mathematical implementation of the simple triangle construction proposed in [3]. The corresponding formulae are quite complicated and are given in [6]. In order to illustrate these contours in a quantitative way, let us assume – in analogy to an example discussed by Neubert and Rosner in [19] – that  $\gamma = 76^\circ$ ,  $r = 0.15$  and  $\delta = 20^\circ$ . If we use, moreover,  $q_C e^{i\omega_C} = 0.66 \times 0.25$  and  $\rho = 0$ , we obtain  $R = 1.00$  and  $A_0 = 9.96\%$ . The contours in the  $\gamma$ - $r$  plane corresponding to these “measured” observables are shown in Fig. 2. For  $r = 0.15$ , which is represented in this figure by the dotted line, we have four solutions for  $\gamma$ :  $19^\circ$ ,  $76^\circ$ , which is the

“true” value in our example,  $85^\circ$  and  $161^\circ$ . Moreover, a range of  $78^\circ \leq \gamma \leq 84^\circ$  is excluded. Since the values of  $19^\circ$  and  $161^\circ$  are outside the presently allowed range of  $41^\circ \lesssim \gamma \lesssim 97^\circ$  [34], which is implied by the usual fits of the unitarity triangle, we are left with the two “physical” solutions of  $76^\circ$  and  $85^\circ$ . In this example, the contours in the  $\gamma$ - $r$  plane have the very interesting feature that these solutions are almost independent of the value of  $r$  (see also [6]). Consequently, they are only affected to a small extent by the uncertainty of  $r$ . As we have already noted, if rescattering processes should play an important role, it may be difficult to fix this parameter in a reliable way. While it is possible to take into account the shift of the contours in the  $\gamma$ - $r$  plane due to large rescattering effects, with the help of the decays  $B^\pm \rightarrow K^\pm K$  and the  $SU(3)$  flavour symmetry [6, 7], there is unfortunately no straightforward approach to accomplish this task also in the determination of  $r$ . In [6], also the uncertainties related to the “colour-suppressed” electroweak penguins were analysed. If we used, for example, the strongly suppressed “factorized” result (29) to deal with these topologies in the contours in the  $\gamma$ - $r$  plane, we would obtain the solutions  $\gamma = 19^\circ, 82^\circ, 91^\circ, 161^\circ$  for  $r = 0.15$ , i.e. our “physical” solutions from above would be shifted by  $6^\circ$  towards larger values of  $\gamma$ .

This example shows nicely that the new central value of  $R = 1$  reported recently by the CLEO collaboration [8] does by no means imply – even if confirmed by future data – that the modes  $B^\pm \rightarrow \pi^\pm K$  and  $B_d \rightarrow \pi^\mp K^\pm$  are “useless” to probe the CKM angle  $\gamma$ . Although the constraints on this angle that are implied by the combined branching ratios of these modes would not be effective in this case (see Fig. 1), the prospects to determine  $\gamma$  as soon as CP violation in  $B_d \rightarrow \pi^\mp K^\pm$  is measured appear to be promising.

## 4 Probing the CKM Angle $\gamma$ with the Charged Decays $B^\pm \rightarrow \pi^\pm K$ and $B^\pm \rightarrow \pi^0 K^\pm$

The subjects of this section are strategies to probe the CKM angle  $\gamma$  with the help of the observables  $R_c$  and  $A_0^c$  defined in (50) and (51). In this context, an important additional ingredient is provided by the fact that the amplitude  $T+C$  can be determined with the help of the decay  $B^+ \rightarrow \pi^+ \pi^0$  by using the  $SU(3)$  flavour symmetry of strong interactions [10]:

$$T + C \approx -\sqrt{2} \frac{V_{us}}{V_{ud}} \frac{f_K}{f_\pi} A(B^+ \rightarrow \pi^+ \pi^0). \quad (65)$$

Here the ratio  $f_K/f_\pi = 1.2$  of the kaon and pion decay constants takes into account factorizable  $SU(3)$ -breaking corrections. At present, the non-factorizable corrections to (65) cannot be treated in a quantitative way. It should be noted that electroweak penguin contributions are also not included in this expression. However, the formalism discussed in Subsection 2.2 applies also to the  $B \rightarrow \pi\pi$  case, where the  $SU(2)$  isospin symmetry suffices to derive the following expression:

$$\left[ \left| \frac{P_{\text{ew}}}{T+C} \right| e^{i(\delta_{\text{ew}} - \delta_{T+C})} \right]_{\bar{b} \rightarrow \bar{d}} = \frac{3}{2R_b} \left[ \frac{C_9(\mu) + C_{10}(\mu)}{C'_1(\mu) + C'_2(\mu)} \right] = -3.3 \times \left[ \frac{0.41}{R_b} \right] \times 10^{-2}. \quad (66)$$



As in the  $\bar{b} \rightarrow \bar{s}$  case, the amplitudes  $(T + C)_{\bar{b} \rightarrow \bar{d}}$  and  $(P_{\text{ew}})_{\bar{b} \rightarrow \bar{d}}$  are proportional to the CKM factors  $\lambda_u^{(d)}$  and  $\lambda_c^{(d)}$ , respectively. Using (66), we find the corrected expression

$$T + C \approx -\sqrt{2} \frac{V_{us}}{V_{ud}} \frac{f_K}{f_\pi} \left[ \frac{A(B^+ \rightarrow \pi^+ \pi^0)}{1 + 0.033 \times e^{-i\gamma}} \right]. \quad (67)$$

Consequently, the electroweak penguins lead to a correction to (65) that is at most a few per cent. It is interesting to note that a theoretical input similar to (66) allows us to include electroweak penguin topologies in the well-known Gronau–London method [35] to determine the angle  $\alpha$  of the unitarity triangle with the help of  $B \rightarrow \pi\pi$  isospin relations. This by-product of our considerations is discussed in more detail in the appendix.

## 4.1 Strategies to Constrain the CKM Angle $\gamma$

The constraints on  $\gamma$  implied by (63) and (64) apply also to the  $B^\pm \rightarrow \pi^\pm K$ ,  $\pi^0 K^\pm$  case, if straightforward replacements are performed. We just have to substitute

$$R \rightarrow R_c, \quad r \rightarrow r_c, \quad q_C e^{i\omega_C} \rightarrow q e^{i\omega} \quad (68)$$

in these expressions, leading to the extremal values

$$R_c^{\text{ext}} \Big|_{\delta_c} = 1 \pm 2 \frac{r_c}{u} \sqrt{h^2 + k^2} + v^2 r_c^2 \quad (69)$$

and

$$R_c^{\text{min}} \Big|_{r_c, \delta_c} = \left[ \frac{1 + 2 q \rho \cos(\theta + \omega) + q^2 \rho^2}{(1 - 2 q \cos \omega \cos \gamma + q^2)(1 + 2 \rho \cos \theta \cos \gamma + \rho^2)} \right] \sin^2 \gamma. \quad (70)$$

Note that also  $q_C e^{i\omega_C}$  has to be replaced by  $q e^{i\omega}$  in the quantities  $h$ ,  $k$  and  $v$  specified in (33)–(36). In comparison with  $B^\pm \rightarrow \pi^\pm K$  and  $B_d \rightarrow \pi^\mp K^\pm$ , the decays  $B^\pm \rightarrow \pi^\pm K$ ,  $\pi^0 K^\pm$  have the advantage that  $r_c$  can be extracted with the help of (65), i.e. by using only the  $SU(3)$  flavour symmetry. The present data give  $r_c = 0.24 \pm 0.06$  [18].

Because of the present experimental range of  $R_c^{\text{exp}} = 2.1 \pm 1.1$ , the bounds on  $\gamma$  associated with (70) are not effective at the moment and the major role to constrain this angle is played by the maximal value of  $R_c$ , which corresponds to “+” in (69). The values of  $\gamma$  implying  $R_c^{\text{exp}} > R_c^{\text{max}}$  are excluded. These constraints correspond to the bound pointed out by Neubert and Rosner in [18], who considered the observable  $R_* = 1/R_c$  and performed an expansion in the parameter  $r_c$  in order to derive their bound. Moreover, rescattering effects were completely neglected, i.e. only the case  $\rho = 0$  was considered, and  $\omega = 0^\circ$  was assumed. In contrast, our result (69) is valid *exactly* and provides a simple interpretation of these constraints on  $\gamma$ . Furthermore, it allows us to investigate the sensitivity both on rescattering and on possible  $SU(3)$ -breaking effects (see (46)–(48)). The latter may, among other things, lead to  $\omega \neq 0^\circ$ .

In Fig. 3, we have chosen  $q e^{i\omega} = 0.63$  to illustrate the constraints on the CKM angle  $\gamma$  that are implied by (69) and (70) for values of  $r_c$  lying within the presently allowed range given in [18]. The thick dot-dashed line corresponds to the leading-order term of

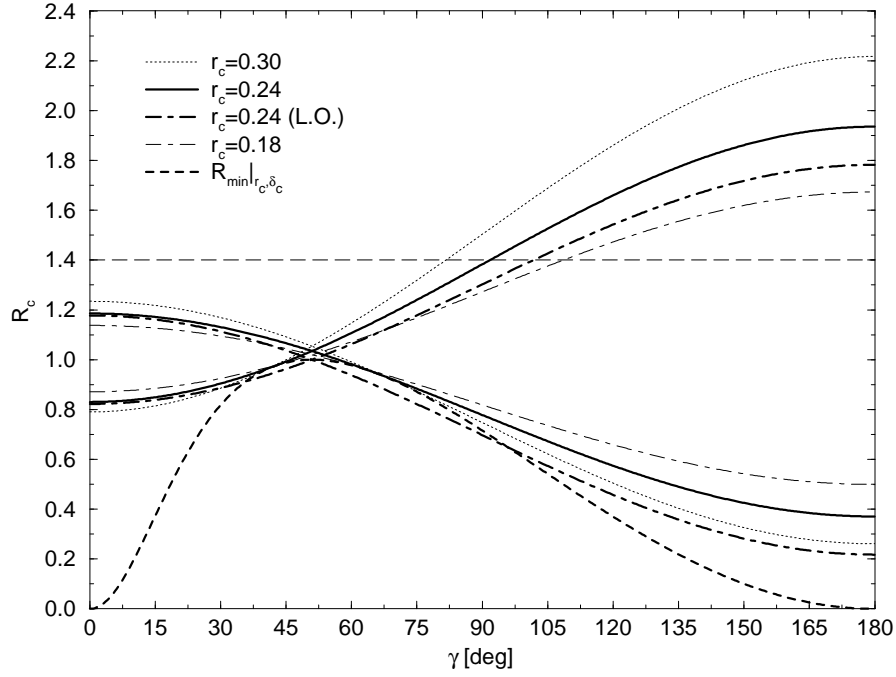


Figure 3: The dependence of the extremal values of  $R_c$  described by (69) and (70) on the CKM angle  $\gamma$  for  $q e^{i\omega} = 0.63$  in the case of negligible rescattering effects, i.e.  $\rho = 0$ .

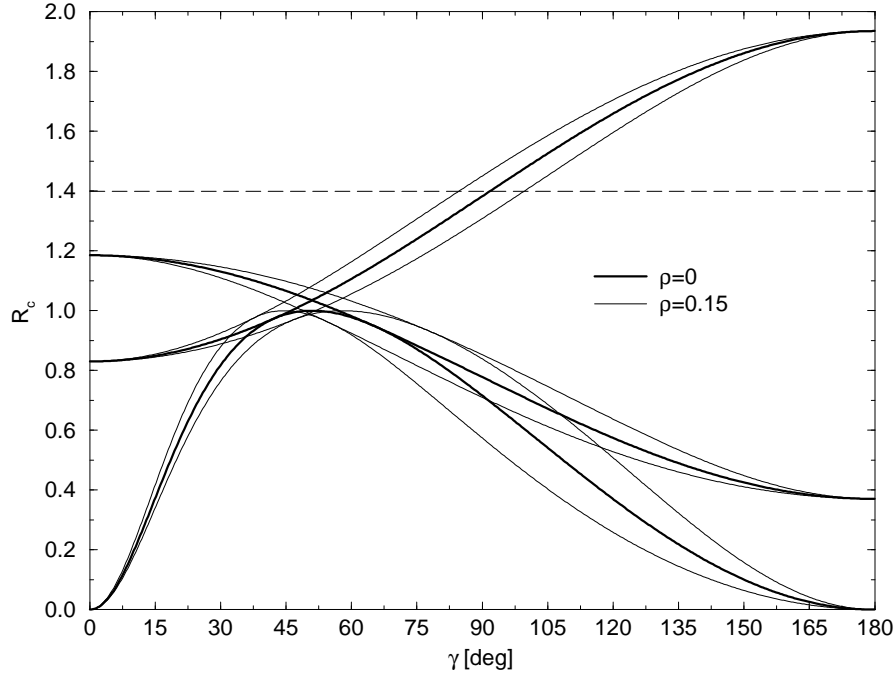


Figure 4: The impact of rescattering effects on the extremal values of  $R_c$  described by (69) and (70) for  $q e^{i\omega} = 0.63$  and  $r_c = 0.24$  ( $\theta \in \{0^\circ, 180^\circ\}$ ).

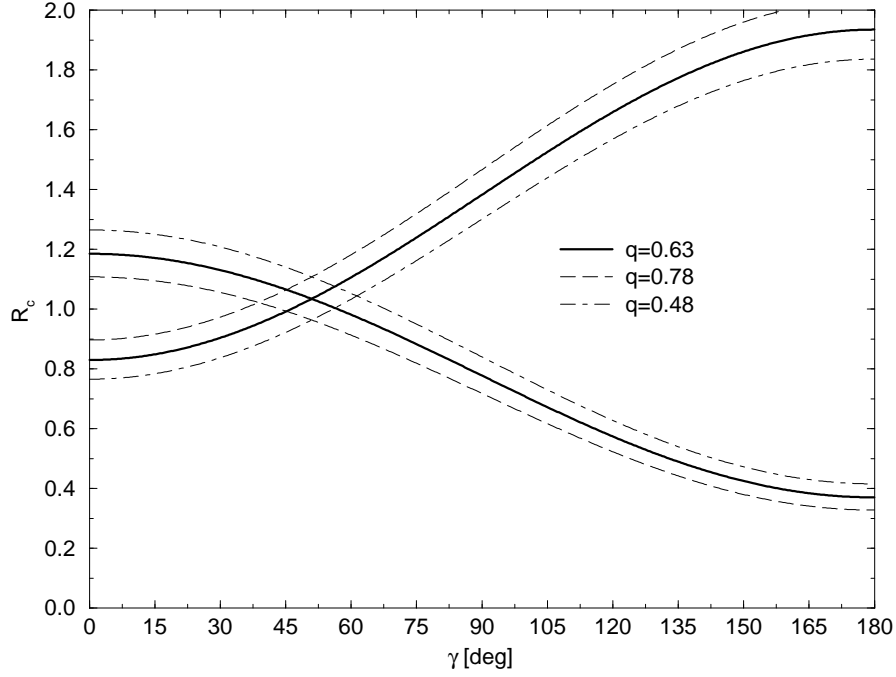


Figure 5: The dependence of the extremal values of  $R_c$  described by (69) on the CKM angle  $\gamma$  for  $r_c = 0.24$ ,  $\omega = 0^\circ$  and for various values of  $q$  ( $\rho = 0$ ).

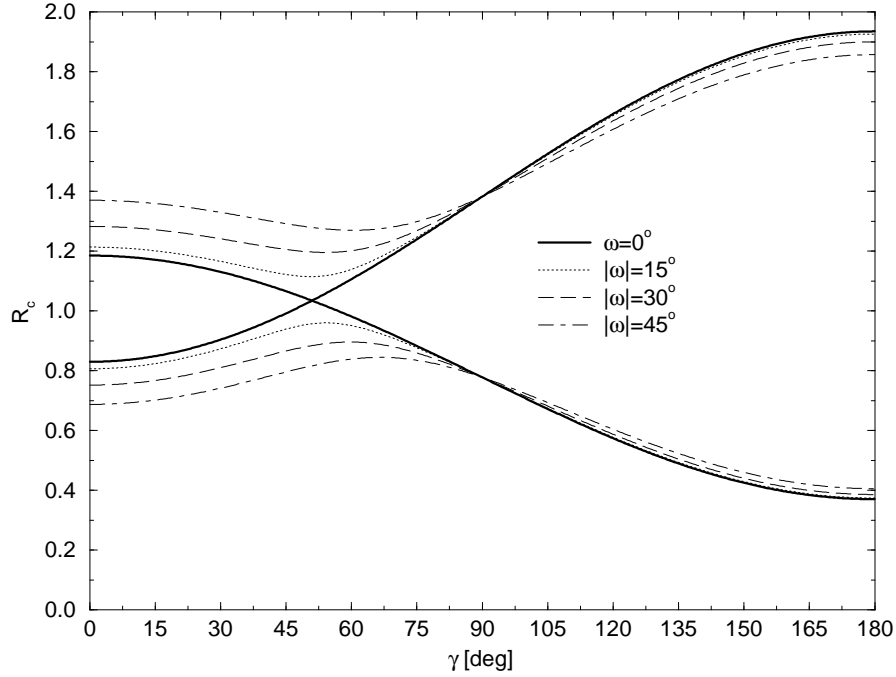


Figure 6: The dependence of the extremal values of  $R_c$  described by (69) on the CKM angle  $\gamma$  for  $r_c = 0.24$ ,  $q = 0.63$  and for various values of  $\omega$  ( $\rho = 0$ ).

the expansion employed by Neubert and Rosner in [18]. In the case of  $r_c = 0.24$  and  $R_c = 1.4$ , values of  $\gamma < 92^\circ$  would be excluded, as can be read off easily from this figure. We observe that the lower bound on  $\gamma$  following from the leading-order result given in [18] receives a sizeable correction of  $-10^\circ$  in this example.

The extraction of the parameter  $r_c$  is – in contrast to the determination of  $r$  in the  $B^\pm \rightarrow \pi^\pm K$ ,  $B_d \rightarrow \pi^\mp K^\pm$  case – not affected by rescattering processes and can be accomplished by using only  $SU(3)$  flavour symmetry arguments. However, this feature does not imply that the constraints on  $\gamma$  are also not affected by rescattering processes, which may lead to sizeable values of  $\rho$ . We have illustrated these effects in Fig. 4, where we have chosen  $qe^{i\omega} = 0.63$ ,  $r_c = 0.24$ ,  $\rho = 0.15$  and  $\theta \in \{0^\circ, 180^\circ\}$ . For these strong phases, the rescattering effects are maximal. In the case of  $R_c = 1.4$ , they lead to an uncertainty of  $\Delta\gamma = \pm 7^\circ$ . If we compare these effects with the analysis performed in [6], we observe that the constraints on  $\gamma$  are affected, to a similar extent, by rescattering processes, as are those implied by the  $B^\pm \rightarrow \pi^\pm K$  and  $B_d \rightarrow \pi^\mp K^\pm$  observables [5]. In our formalism, these effects can be taken into account with the help of the strategies proposed in [6, 7] (for alternative methods, see [22, 25]). To this end, additional experimental data provided by  $B^\pm \rightarrow K^\pm K$  decays are needed. Since this issue was discussed extensively in [6, 7], we will not work it out in more detail here.

Let us now investigate the uncertainties associated with the electroweak penguin parameter  $qe^{i\omega}$ . In Fig. 5, we show the dependence of (69) on the CKM angle  $\gamma$  for  $r_c = 0.24$ ,  $\omega = 0^\circ$  and for various values of  $q$ . The strong phase  $\omega$  is varied in Fig. 6 by keeping  $r_c = 0.24$  and  $q = 0.63$  fixed. If we look at these figures, we observe that in particular non-vanishing values of  $\omega$ , which may be induced by non-factorizable  $SU(3)$ -breaking effects, may weaken the bounds on  $\gamma$  implied by (69) significantly for  $1.2 \lesssim R_c \lesssim 1.4$ . As we will see in the next subsection, a similar comment applies to the strategies to determine the CKM angle  $\gamma$  with the help of the decays  $B^\pm \rightarrow \pi^\pm K$ ,  $\pi^0 K^\pm$ .

## 4.2 Strategies to Determine the CKM Angle $\gamma$

In analogy to the  $B^\pm \rightarrow \pi^\pm K$ ,  $B_d \rightarrow \pi^\mp K^\pm$  strategy, it is possible to go beyond the bounds on  $\gamma$  discussed in the previous subsection as soon as CP violation in  $B^\pm \rightarrow \pi^0 K^\pm$  decays is observed. We then are in a position to determine contours in the  $\gamma$ - $r_c$  plane with the help of the general formulae given in [6]. Since  $r_c$  can be fixed through (65),  $\gamma$  can be determined from these contours, which correspond to a mathematical implementation of the simple triangle construction proposed in [10]. However, in contrast to this construction, these contours take into account electroweak penguins through (48).

Let us consider again a specific example in order to illustrate this strategy in more detail. To this end, we follow Neubert and Rosner [19] and assume that  $\gamma = 76^\circ$ ,  $\rho = 0$ ,  $r_c = 0.24$ ,  $\delta_c = 20^\circ$  and  $qe^{i\omega} = 0.63$  to calculate the observables  $R_c$  and  $A_0^c$ . These parameters give  $R_c = 1.24$  and  $A_0^c = 15.9\%$ . In Fig. 7, we show the corresponding contours in the  $\gamma$ - $r_c$  plane. The thick lines describe the contours arising for  $\rho = 0$ , and the dotted line represents the “measured” value of  $r_c$ . Their intersection gives a two-fold solution for  $\gamma$ , including the “true” value of  $76^\circ$  and a second solution of  $160^\circ$ .

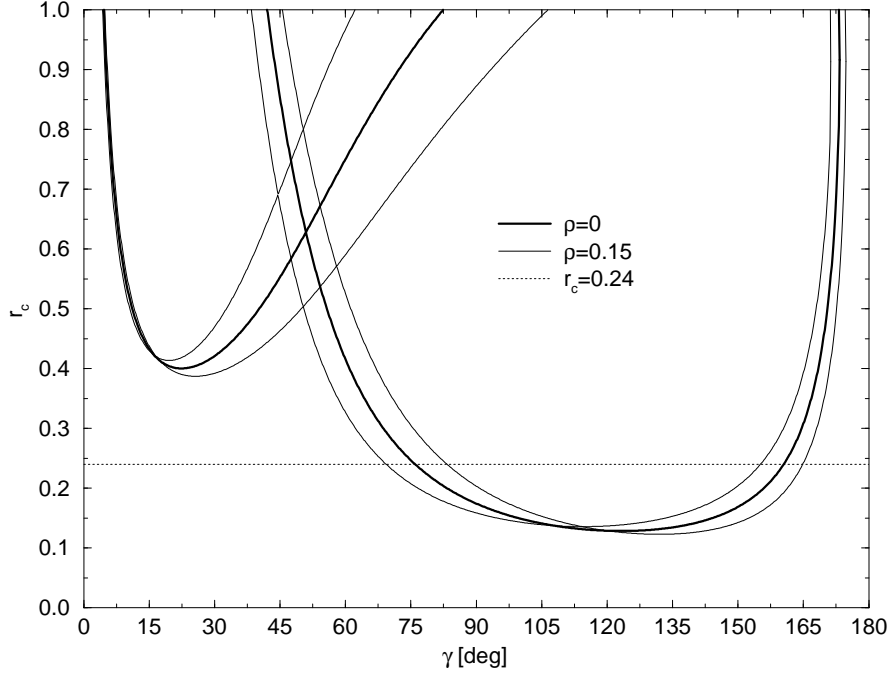


Figure 7: The contours in the  $\gamma$ - $r_c$  plane corresponding to  $R_c = 1.24$ ,  $A_0^c = 15.9\%$  and  $q e^{i\omega} = 0.63$ . The thin lines illustrate rescattering effects ( $\rho = 0.15$ ,  $\theta \in \{0^\circ, 180^\circ\}$ ).

The thin lines illustrate the impact of possible rescattering processes and are obtained for  $\rho = 0.15$  and  $\theta \in \{0^\circ, 180^\circ\}$ . For these strong phases, the rescattering effects are maximal. Applying the strategies proposed in [6, 7], the rescattering effects can be taken into account in these contours. To this end, additional experimental data on  $B^\pm \rightarrow K^\pm K$  decays are required. Unfortunately, non-factorizable  $SU(3)$ -breaking effects cannot be included in a similar manner. Let us emphasize again at this point that such corrections may affect both the determination of  $|T + C|$ , i.e. of  $r_c$ , and the calculation of the electroweak penguin parameter  $q e^{i\omega}$ , which may therefore be shifted significantly from (48). In Fig. 8, we show the dependence of the contours in the  $\gamma$ - $r_c$  plane arising in our specific example on the parameter  $q$ , while we illustrate the impact of non-vanishing values of the strong phase  $\omega$  in Fig. 9. In these two figures, we have neglected rescattering effects, i.e. we have chosen  $\rho = 0$ . We observe that the contours are rather sensitive to the phase  $\omega$ . For values of  $\omega = -30^\circ$ , we even get additional solutions for  $\gamma$ .

Before we present a new strategy to probe the CKM angle  $\gamma$  with the help of the neutral decays  $B_d \rightarrow \pi^0 K$ ,  $\pi^\mp K^\pm$ , let us briefly go back to the  $B^\pm \rightarrow \pi^\pm K$ ,  $B_d \rightarrow \pi^\mp K^\pm$  approach discussed in Section 3. If we compare the contours in the  $\gamma$ - $r$  plane shown in Fig. 2 with those in the  $\gamma$ - $r_c$  plane shown in Fig. 7, we observe that they are very different from each other. In particular, the  $B^\pm \rightarrow \pi^\pm K$ ,  $B_d \rightarrow \pi^\mp K^\pm$  case appears to be more promising for this specific example. Time will tell which one of these two strategies is really more powerful in practice.

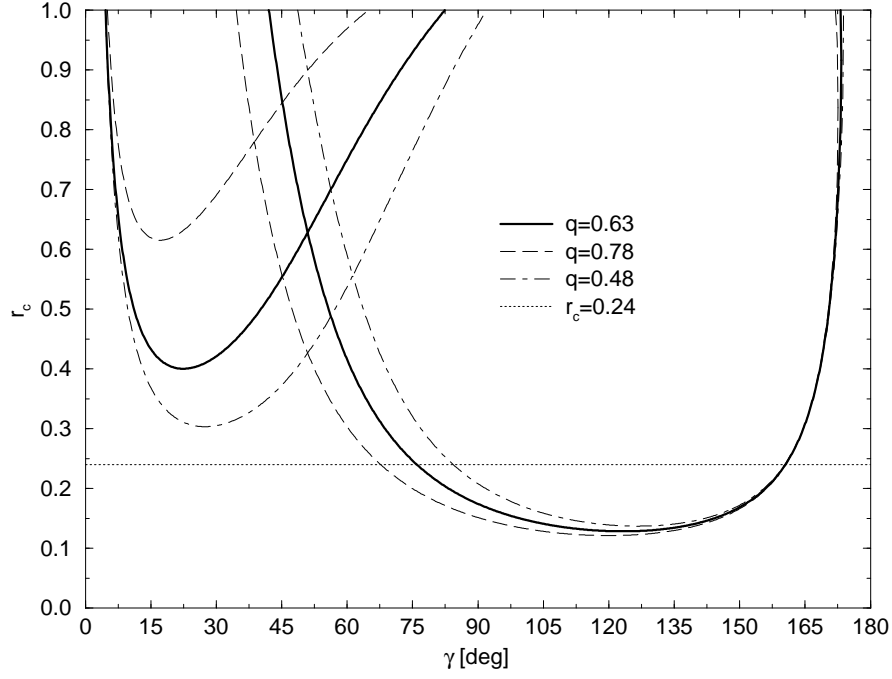


Figure 8: The dependence of the contours in the  $\gamma$ - $r_c$  plane corresponding to  $R_c = 1.24$ ,  $A_0^c = 15.9\%$  and  $\omega = 0^\circ$  on the parameter  $q$  ( $\rho = 0$ ).

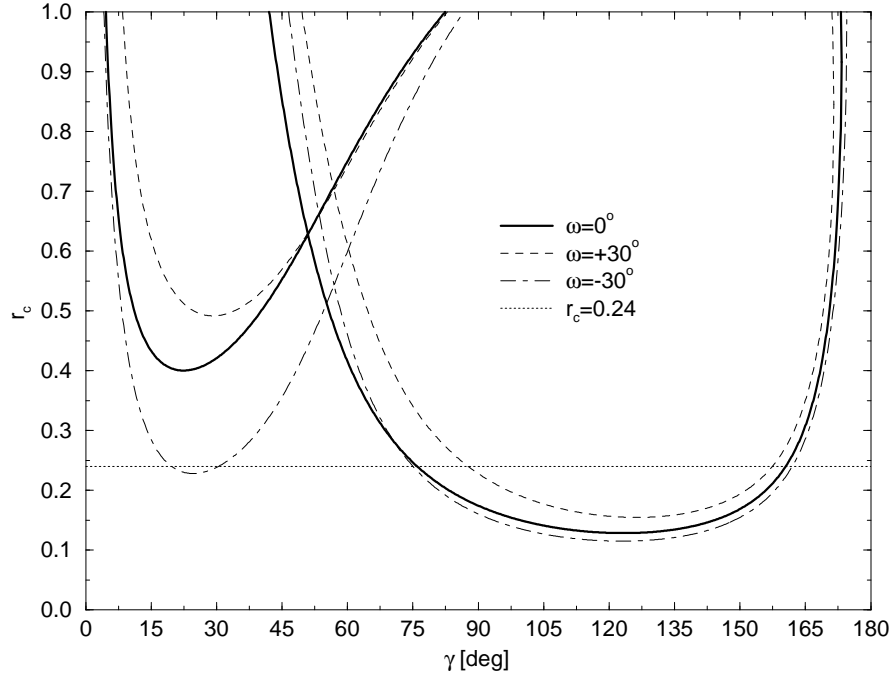


Figure 9: The impact of non-vanishing values of the strong phase  $\omega$  on the contours in the  $\gamma$ - $r_c$  plane corresponding to  $R_c = 1.24$ ,  $A_0^c = 15.9\%$  and  $q = 0.63$  ( $\rho = 0$ ).

## 5 Probing the CKM Angle $\gamma$ with the Neutral Decays $B_d \rightarrow \pi^0 K$ and $B_d \rightarrow \pi^\mp K^\pm$

The observables  $R_n$  and  $A_0^n$  of the neutral  $B$  decays  $B_d \rightarrow \pi^0 K$ ,  $\pi^\mp K^\pm$  allow strategies to probe the CKM angle  $\gamma$  that are completely analogous to those discussed in the previous section. However, in the case of these modes, we have an additional CP-violating observable at our disposal, which allows us to take into account rescattering effects in a theoretically clean way. The point is as follows: since  $B_d \rightarrow \pi^\mp K^\pm$  is a self-tagging neutral  $B$  decay, it exhibits only direct CP violation due to the interference between the “tree” and “penguin” amplitudes, but no mixing-induced CP violation, arising from interference effects between  $B_d^0$ – $\overline{B}_d^0$  mixing and decay processes. On the other hand, if we consider  $B_d \rightarrow \pi^0 K$  modes and require that the kaon be observed as a  $K_S$ , the resulting final state  $f$  is an eigenstate of the CP operator with eigenvalue  $-1$ . In this case, we have to deal with mixing-induced CP violation and obtain the following time-dependent CP asymmetry [36]:

$$\begin{aligned} A_{\text{CP}}(B_d(t) \rightarrow f) &\equiv \frac{\Gamma(B_d^0(t) \rightarrow f) - \Gamma(\overline{B}_d^0(t) \rightarrow f)}{\Gamma(B_d^0(t) \rightarrow f) + \Gamma(\overline{B}_d^0(t) \rightarrow f)} \\ &= \mathcal{A}_{\text{CP}}^{\text{dir}}(B_d \rightarrow f) \cos(\Delta M_d t) + \mathcal{A}_{\text{CP}}^{\text{mix-ind}}(B_d \rightarrow f) \sin(\Delta M_d t). \end{aligned} \quad (71)$$

Here  $\Gamma(B_d^0(t) \rightarrow f)$  and  $\Gamma(\overline{B}_d^0(t) \rightarrow f)$  denote the decay rates of initially, i.e. at time  $t = 0$ , present  $B_d^0$  and  $\overline{B}_d^0$  mesons, respectively;  $\Delta M_d$  is the mass difference of the  $B_d$  mass eigenstates, and

$$\mathcal{A}_{\text{CP}}^{\text{dir}}(B_d \rightarrow f) = \frac{1 - |\xi_f^{(d)}|^2}{1 + |\xi_f^{(d)}|^2} \quad (72)$$

$$\mathcal{A}_{\text{CP}}^{\text{mix-ind}}(B_d \rightarrow f) = \frac{2 \text{Im} \xi_f^{(d)}}{1 + |\xi_f^{(d)}|^2} \quad (73)$$

describe direct and mixing-induced CP violation. The observable  $\xi_f^{(d)}$  containing essentially all the information needed to evaluate these CP-violating asymmetries is given as follows:

$$\xi_f^{(d)} = \mp e^{-i\phi_M^{(d)}} \frac{A(\overline{B}_d^0 \rightarrow f)}{A(B_d^0 \rightarrow f)}, \quad (74)$$

where  $A(B_d^0 \rightarrow f)$  and  $A(\overline{B}_d^0 \rightarrow f)$  are “unmixed” decay amplitudes,  $\phi_M^{(d)} = 2 \arg(V_{td}^* V_{tb})$  denotes the weak  $B_d^0$ – $\overline{B}_d^0$  mixing phase, and  $(\mathcal{CP})|f\rangle = \pm|f\rangle$ . If the final state  $f$  contains a neutral kaon, as in the case of  $B_d \rightarrow \pi^0 K_S$ , we have in addition to take into account a phase  $\phi_K$ , which is related to  $K^0$ – $\overline{K}^0$  mixing and is negligibly small in the Standard Model. The combination  $\phi_M^{(d)} + \phi_K$ , which is relevant for  $B_d \rightarrow \pi^0 K_S$ , can be determined in a theoretically clean way with the help of the “gold-plated” mode  $B_d \rightarrow J/\psi K_S$  [37]:

$$A_{\text{CP}}(B_d(t) \rightarrow J/\psi K_S) = - \sin(\phi_M^{(d)} + \phi_K) \sin(\Delta M_d t). \quad (75)$$

Within the Standard Model, we have  $\phi_M^{(d)} = 2\beta$ , where  $\beta$  is another angle of the unitarity triangle, and  $\phi_K = 0$  to a very good approximation. In the case of the decay  $B_d \rightarrow \pi^0 K_S$ , the observables (72) and (73) can be expressed as follows [38, 39]:

$$\mathcal{A}_{\text{CP}}^{\text{dir}}(B_d \rightarrow \pi^0 K_S) = \frac{|P_n|^2 - |\overline{P}_n|^2}{|P_n|^2 + |\overline{P}_n|^2} \quad (76)$$

$$\mathcal{A}_{\text{CP}}^{\text{mix-ind}}(B_d \rightarrow \pi^0 K_S) = -\frac{2|P_n||\overline{P}_n|}{|P_n|^2 + |\overline{P}_n|^2} \sin \left[ \left( \phi_M^{(d)} + \phi_K \right) + \psi \right], \quad (77)$$

where  $P_n \equiv \sqrt{2} A(B_d^0 \rightarrow \pi^0 K^0)$  (see (60)),  $\overline{P}_n \equiv \sqrt{2} A(\overline{B}_d^0 \rightarrow \pi^0 \overline{K}^0)$ , and  $\psi$  denotes the angle between these amplitudes, i.e.  $\overline{P}_n/P_n \equiv e^{-i\psi} |\overline{P}_n|/|P_n|$ .

The determination of  $\gamma$  by means of  $B_d \rightarrow \pi^0 K$ ,  $\pi^\mp K^\pm$ , which we would like to propose here, uses Eqs. (39), (48), (65), (71) and (75)–(77). The geometrical version of this determination, which is illustrated in Fig. 10, proceeds in the following steps:

1. From time-dependent studies of the  $B_d \rightarrow \pi^0 K_S$  and  $B_d \rightarrow J/\psi K_S$  decay rates and the associated CP-violating asymmetries, which are represented by (71) and (75)–(77), we determine the absolute values of the amplitudes  $P_n$  and  $\overline{P}_n$ , as well as their relative orientation in the complex plane, i.e. the angle  $\psi$ .
2. Using (48) and (65), we determine  $|P_{\text{ew}}|$  and  $|T + C| = |\overline{T} + \overline{C}|$ , respectively.
3. Using  $\text{BR}(B_d^0 \rightarrow \pi^- K^+)$  and  $\text{BR}(\overline{B}_d^0 \rightarrow \pi^+ K^-)$ , we determine the magnitudes of the amplitudes  $A \equiv A(B_d^0 \rightarrow \pi^- K^+)$  and  $\overline{A} \equiv A(\overline{B}_d^0 \rightarrow \pi^+ K^-)$ , respectively.
4. The information collected in steps 1–3 allows us to construct two quadrangles in the complex plane, as shown in Fig. 10. They are a geometrical representation of the amplitude relation (39) and its CP conjugate, which – in terms of the notation used in this figure – take the form

$$P_n + (T + C) + A + P_{\text{ew}} = 0 \quad (78)$$

$$\overline{P}_n + (\overline{T} + \overline{C}) + \overline{A} + P_{\text{ew}} = 0. \quad (79)$$

Since only information on  $|P_{\text{ew}}|$  has been used so far, the precise shapes of these two quadrangles are not yet fixed.

5. Finally, we make again use of (48) to determine the phase  $\omega = \delta_{\text{ew}} - \delta_{T+C}$ . This gives us the orientation of the electroweak penguin amplitude  $P_{\text{ew}}$  with respect to the line that bisects the angle between  $T + C$  and  $\overline{T} + \overline{C}$ . This final information, together with the construction of step 4, determines the shapes of the two quadrangles in question, and consequently also the CKM angle  $\gamma$ , as shown in Fig. 10.

In this construction, there are no uncertainties due to rescattering effects, and the theoretical accuracy is limited only by non-factorizable  $SU(3)$ -breaking corrections, which may affect (48) and (65).



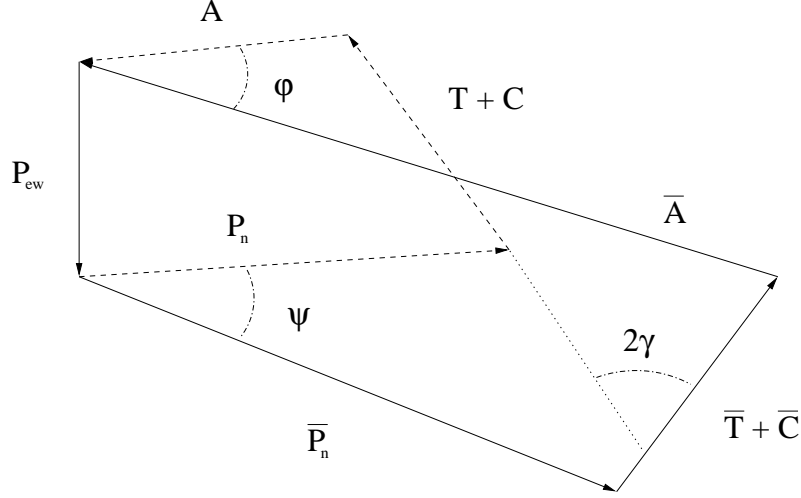


Figure 10: Illustration of a strategy to determine the CKM angle  $\gamma$  by means of the neutral decays  $B_d^0 \rightarrow \pi^0 K^0$ ,  $B_d^0 \rightarrow \pi^- K^+$  and their charge conjugates.

In order to have the tools available to implement this geometrical construction in a mathematical way, we give the explicit expression for  $\mathcal{A}_{\text{CP}}^{\text{mix-ind}}(B_d \rightarrow \pi^0 K_S)$  in terms of the parameters  $\rho_n$  and  $\theta_n$  defined in (60):

$$\mathcal{A}_{\text{CP}}^{\text{mix-ind}}(B_d \rightarrow \pi^0 K_S) = - \left[ \frac{\sin(\phi_M^{(d)} + \phi_K) + 2\rho_n \cos\theta_n \sin(\phi_M^{(d)} + \phi_K + \gamma) + \rho_n^2 \sin(\phi_M^{(d)} + \phi_K + 2\gamma)}{1 + 2\rho_n \cos\theta_n \cos\gamma + \rho_n^2} \right], \quad (80)$$

which reduces to

$$\mathcal{A}_{\text{CP}}^{\text{mix-ind}}(B_d \rightarrow \pi^0 K_S) = -\sin(\phi_M^{(d)} + \phi_K) = \mathcal{A}_{\text{CP}}^{\text{mix-ind}}(B_d \rightarrow J/\psi K_S) \quad (81)$$

in the case of  $\rho_n = 0$  [3]. The direct CP asymmetry  $\mathcal{A}_{\text{CP}}^{\text{dir}}(B_d \rightarrow \pi^0 K_S)$  takes the same form as the direct CP asymmetry  $A_+$  arising in the decay  $B^+ \rightarrow \pi^+ K^0$  (see (38)). Consequently, measuring  $\mathcal{A}_{\text{CP}}^{\text{dir}}(B_d \rightarrow \pi^0 K_S)$ ,  $\mathcal{A}_{\text{CP}}^{\text{mix-ind}}(B_d \rightarrow \pi^0 K_S)$ ,  $R_n$  and  $A_0^n$  (see (55) and (56)), we can determine the four “unknowns”  $\rho_n$ ,  $\theta_n$ ,  $\delta_n$  and the CKM angle  $\gamma$  ( $r_n$  and  $\phi_M^{(d)} + \phi_K$  are fixed through (65) and (75), respectively) as functions of the electroweak penguin parameter  $q e^{i\omega}$ . The latter can be determined by using (48).

The utility of time-dependent measurements of the decay  $B_d \rightarrow \pi^0 K_S$  to probe angles of the unitarity triangle was already pointed out several years ago by Nir and Quinn [30], who proposed a strategy to determine the angle  $\alpha$  with the help of the amplitude relation (39). At that time, it was believed that electroweak penguins play only a very minor role in  $B$  decays, which is actually not the case because of the large top-quark mass [13, 14]. A construction similar to the one shown in Fig. 10 would in fact allow the extraction of

the CKM angle  $\alpha$ , if electroweak penguins played a negligible role, i.e. if  $P_{\text{ew}} = 0$ . In order to see how this strategy works, we have to rotate the CP-conjugate amplitudes  $\overline{P}_n$ ,  $\overline{T} + \overline{C}$  and  $\overline{A}$  by the phase factor  $e^{-i(\phi_M^{(d)} + \phi_K)} = e^{-i2\beta}$ , so that the angle between  $T + C$  and the rotated  $\overline{T} + \overline{C}$  amplitude is a measure of  $2\alpha$  (note that  $\beta + \gamma = 180^\circ - \alpha$ ). A similar “trick” was also used in our discussion of the  $B \rightarrow \pi\pi$  approach given in the appendix. Since the angle  $\tilde{\psi} \equiv (\phi_M^{(d)} + \phi_K) + \psi$  between  $P_n$  and the rotated amplitude  $\overline{P}_n$  can be determined directly by using the mixing-induced CP asymmetry (77), the CKM angle  $\alpha$  can be determined. Unfortunately, this construction does not work in the presence of electroweak penguins. In order to take them into account with the help of (48), the phase  $\phi_M^{(d)} + \phi_K$  of the rotated electroweak penguin amplitude  $\overline{P}_{\text{ew}} (= P_{\text{ew}})$  has to be determined by making use of (75), and we arrive at a construction, which is equivalent to the one discussed above. Interestingly, the situation in this respect is very different in the  $\alpha$  determination from  $B \rightarrow \pi\pi$  isospin triangle relations, as we show in the appendix.

Let us now come back to the decay  $B_d \rightarrow \pi^0 K$ . Concerning the parameter  $\rho_n$  defined in (61), the usual naïve expectation based on “colour suppression” and “short-distance” arguments is a value at the level of a few per cent, implying small direct CP violation in  $B_d \rightarrow \pi^0 K$  and small corrections to (81). Moreover, we would expect a tiny angle  $\psi$  between the amplitudes  $P_n$  and  $\overline{P}_n$  in Fig. 10. However, rescattering effects of the kind discussed in [16], [20]–[24] may in principle also lead to an enhancement of  $\rho_n$ , thereby affecting (81) and leading to sizeable direct CP violation in  $B_d \rightarrow \pi^0 K$ , as well as to a sizeable value of the angle  $\psi$ . On the other hand, if (76) and (77) should in fact imply a tiny value of  $\psi$ , i.e. that  $P_n \approx \overline{P}_n$ , there would be a simple strategy to extract  $\gamma$  by using in addition the observables provided by an analysis of the decay  $B_s \rightarrow K^+ K^-$ . For sizeable values of  $\psi$ , this mode would also be very useful, allowing us to reduce the theoretical input concerning the electroweak penguins considerably. Let us turn to this decay in the following section.

## 6 Strategies to Combine $B_s \rightarrow K^+ K^-$ Modes with $B_{u,d} \rightarrow \pi K$ Decays

### 6.1 Preliminaries

The decay  $B_s \rightarrow K^+ K^-$ , which is the  $B_s$  counterpart of the mode  $B_d \rightarrow \pi^\mp K^\pm$ , plays an important role to probe the CKM angle  $\gamma$  and to obtain experimental insights into electroweak penguins [3, 17, 39–41]. In contrast to the  $B_d$  case, there may be a sizeable width difference  $\Delta\Gamma_s \equiv \Gamma_H^{(s)} - \Gamma_L^{(s)}$  between the mass eigenstates  $B_s^H$  (“heavy”) and  $B_s^L$  (“light”) of the  $B_s$  system [42], which may allow studies of CP violation with untagged  $B_s$  data samples, where one does not distinguish between initially, i.e. at time  $t = 0$ , present  $B_s^0$  or  $\overline{B}_s^0$  mesons [43]. The corresponding untagged  $B_s$  decay rates are defined by

$$\Gamma[f(t)] \equiv \Gamma(B_s^0(t) \rightarrow f) + \Gamma(\overline{B}_s^0(t) \rightarrow f), \quad (82)$$

and can be expressed as (see, for instance, [36])

$$\Gamma[f(t)] \propto [1 + \mathcal{A}_{\Delta\Gamma}(B_s \rightarrow f)] e^{-\Gamma_H^{(s)} t} + [1 - \mathcal{A}_{\Delta\Gamma}(B_s \rightarrow f)] e^{-\Gamma_L^{(s)} t} \quad (83)$$

with

$$\mathcal{A}_{\Delta\Gamma}(B_s \rightarrow f) = \frac{2 \operatorname{Re} \xi_f^{(s)}}{1 + |\xi_f^{(s)}|^2}. \quad (84)$$

Note that there are no rapid oscillatory  $\Delta M_s t$  terms present in (83). The observable  $\xi_f^{(s)}$  is defined in analogy to (74); we have just to replace the  $B_d^0 - \overline{B}_d^0$  mixing phase  $\phi_M^{(d)}$  in that expression by its  $B_s$  counterpart  $\phi_M^{(s)} = 2 \arg(V_{ts}^* V_{tb})$ , which is negligibly small in the Standard Model. The width difference  $\Delta\Gamma_s$  modifies also the expression for the time-dependent CP asymmetry (71). In the  $B_s$  case, it takes the following form:

$$\begin{aligned} A_{\text{CP}}(B_s(t) \rightarrow f) &\equiv \frac{\Gamma(B_s^0(t) \rightarrow f) - \Gamma(\overline{B}_s^0(t) \rightarrow f)}{\Gamma(B_s^0(t) \rightarrow f) + \Gamma(\overline{B}_s^0(t) \rightarrow f)} \\ &= 2 e^{-\Gamma_s t} \left[ \frac{\mathcal{A}_{\text{CP}}^{\text{dir}}(B_s \rightarrow f) \cos(\Delta M_s t) + \mathcal{A}_{\text{CP}}^{\text{mix-ind}}(B_s \rightarrow f) \sin(\Delta M_s t)}{e^{-\Gamma_H^{(s)} t} + e^{-\Gamma_L^{(s)} t} + \mathcal{A}_{\Delta\Gamma}(B_s \rightarrow f) (e^{-\Gamma_H^{(s)} t} - e^{-\Gamma_L^{(s)} t})} \right], \end{aligned} \quad (85)$$

where  $\mathcal{A}_{\text{CP}}^{\text{dir}}(B_s \rightarrow f)$  and  $\mathcal{A}_{\text{CP}}^{\text{mix-ind}}(B_s \rightarrow f)$  correspond to (72) and (73), respectively, and  $\Gamma_s \equiv (\Gamma_H^{(s)} + \Gamma_L^{(s)})/2$ .

If we introduce the notation  $A_s \equiv A(B_s^0 \rightarrow K^+ K^-)$ ,  $\overline{A}_s \equiv A(\overline{B}_s^0 \rightarrow K^+ K^-)$  and denote the angle between these amplitudes by  $\varphi_s$ , we obtain the following expressions for the  $B_s \rightarrow K^+ K^-$  observables [39]:

$$\mathcal{A}_{\text{CP}}^{\text{dir}}(B_s \rightarrow K^+ K^-) = \frac{|A_s|^2 - |\overline{A}_s|^2}{|A_s|^2 + |\overline{A}_s|^2} \quad (86)$$

$$\mathcal{A}_{\text{CP}}^{\text{mix-ind}}(B_s \rightarrow K^+ K^-) = \frac{2 |A_s| |\overline{A}_s|}{|A_s|^2 + |\overline{A}_s|^2} \sin(\phi_M^{(s)} + \varphi_s) \quad (87)$$

$$\mathcal{A}_{\Delta\Gamma}(B_s \rightarrow K^+ K^-) = - \frac{2 |A_s| |\overline{A}_s|}{|A_s|^2 + |\overline{A}_s|^2} \cos(\phi_M^{(s)} + \varphi_s). \quad (88)$$

The measurement of these quantities allows us to construct the amplitudes  $A_s$  and  $\overline{A}_s$  in the complex plane, i.e. to determine both their magnitudes and their relative orientation, provided the  $B_s^0 - \overline{B}_s^0$  mixing phase  $\phi_M^{(s)}$  is known. As we already noted, this phase is tiny in the Standard Model. It can in principle be determined with the help of the decay  $B_s \rightarrow J/\psi \phi$  (see, for example, [40, 44]), which is the  $B_s$  counterpart of the “gold-plated” mode  $B_d \rightarrow J/\psi K_S$  and is very accessible at future hadron machines, for example at the LHC. Large CP violation in  $B_s \rightarrow J/\psi \phi$  would indicate new-physics contributions to  $B_s^0 - \overline{B}_s^0$  mixing. Even in such a scenario of new physics, it would be possible to fix the

amplitudes  $A_s$  and  $\overline{A}_s$  in the complex plane by measuring in addition to (86)–(88) the observables of the decay  $B_s \rightarrow J/\psi \phi$ .

The decays  $B_s \rightarrow K^+ K^-$  and  $B_d \rightarrow \pi^\mp K^\pm$  differ only in their “spectator” quarks and can be related to each other through  $SU(3)$  flavour symmetry arguments. Potential  $SU(3)$ -breaking effects are also due to “penguin annihilation” processes, which contribute to  $B_s \rightarrow K^+ K^-$  (for an explicit expression of the decay amplitude, see [39]), and are absent in  $B_d \rightarrow \pi^\mp K^\pm$ . The importance of these topologies, which are expected to play a minor role [31, 45], can be investigated with the help of the decay  $B_s \rightarrow \pi^+ \pi^-$ ; other interesting probes for  $SU(3)$ -breaking effects can be obtained by comparing the observables of the untagged  $B_s \rightarrow K^+ K^-$  rate with the combined  $B_d \rightarrow \pi^\mp K^\pm$  branching ratio, or their direct CP asymmetries [39]. Let us assume in the following that explorations of this kind indicate small  $SU(3)$ -breaking effects. Then we may identify the angle  $\varphi_s$  between the  $B_s \rightarrow K^+ K^-$  amplitudes  $A_s$  and  $\overline{A}_s$  with the angle  $\varphi$  between the  $B_d \rightarrow \pi^\mp K^\pm$  amplitudes  $A$  and  $\overline{A}$  (see Fig. 10). The knowledge of this angle would be very useful, since it allows us to fix the relative orientation of  $A$  and  $\overline{A}$ .

Let us note that a time-dependent, tagged  $B_s \rightarrow K^+ K^-$  analysis has to be performed in order to determine  $\varphi_s$ . However, if we use the direct CP asymmetry  $A_{\text{CP}}(B_d \rightarrow \pi^\mp K^\pm)$ , the ratio  $|\overline{A}_s|/|A_s|$  can be fixed with the help of the  $SU(3)$  flavour symmetry, allowing the determination of  $\varphi_s$  up to a two-fold ambiguity from the untagged observable (88). Although future  $B$ -physics experiments performed at hadron machines should be in a position to resolve the rapid oscillatory  $\Delta M_s t$  terms arising in tagged  $B_s$  data samples, untagged studies are more promising in terms of efficiency, acceptance and purity [43].

## 6.2 Strategy A

If the angle  $\varphi$  in Fig. 10 is known, the theoretical input concerning the electroweak penguin amplitude  $P_{\text{ew}}$  can be reduced considerably. In particular, step 5 of the procedure given in the previous section could be avoided, since the first four steps, together with the knowledge of the angle  $\varphi$ , would determine the shapes of the two quadrangles in Fig. 10. This would not only allow us to determine the CKM angle  $\gamma$ , but also the strong phase  $\omega$  in (48). Conversely, we could use  $\omega$  as our theoretical input to deal with the electroweak penguins, and could then determine both the electroweak penguin parameter  $q$  and the CKM angle  $\gamma$ . Both approaches would offer some consistency checks for (48).

Should it become possible to determine the CKM angle  $\gamma$  with the help of other strategies, using for example the theoretically clean approach provided by the “tree” decays  $B_s \rightarrow D_s^\pm K^\mp$  [46], the geometrical construction shown in Fig. 10 would allow us to determine the electroweak penguin amplitude  $P_{\text{ew}}$  completely, i.e. both  $q$  and  $\omega$  (see also [17]). To accomplish this task, a sizeable angle  $\psi$  between the amplitudes  $P_n$  and  $\overline{P}_n$  is required. Consequently, this strategy to determine the electroweak penguin amplitude does not work in the case of small rescattering effects and significant “colour suppression” in  $B_d \rightarrow \pi^0 K$ , leading to  $P_n \approx \overline{P}_n$ . As we will see in the next subsection, there is, however, another, simpler strategy to obtain insights into electroweak penguins in this case.

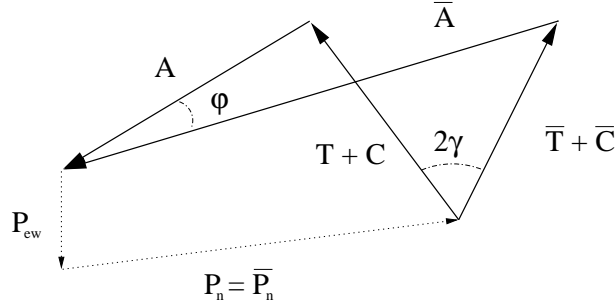


Figure 11: Simple strategy to determine  $\gamma$  with the help of the decays  $B^\pm \rightarrow \pi^\pm \pi^0$ ,  $B_d \rightarrow \pi^\mp K^\pm$  and  $B_s \rightarrow K^+ K^-$  in the case of  $P_n = \overline{P}_n$  (thick solid lines), and to obtain insights into electroweak penguins by using in addition  $B_d \rightarrow \pi^0 K$  (thin dotted lines).

### 6.3 Strategy B

The case  $P_n \approx \overline{P}_n$  would be very favourable for the extraction of  $\gamma$ , thereby offering a new way to determine this angle that is only affected to a small extent by electroweak penguins. For  $P_n = \overline{P}_n$ , there would be no electroweak penguin uncertainties at all. This strategy requires only the measurement of  $B^+ \rightarrow \pi^+ \pi^0$  to fix  $|T+C|$  with the help of (65), and analyses of the decays  $B_d \rightarrow \pi^\mp K^\pm$  and  $B_s \rightarrow K^+ K^-$  to determine the amplitudes  $A$  and  $\overline{A}$  in the complex plane. Although it is possible to see already in Fig. 10 how this  $SU(3)$  strategy works, we think it useful to redraw it for the special case of  $P_n = \overline{P}_n$  in Fig. 11. Here the CKM angle  $\gamma$  can be determined with the help of the simple geometrical construction involving only the thick solid lines. The  $B_d \rightarrow \pi^0 K$  amplitude allows us, furthermore, to fix the electroweak penguin parameter  $q$ , if  $\omega$  is used as an input, or the strong phase  $\omega$ , if we use  $q$  as an input, thereby providing consistency checks for (48).

### 6.4 Strategy C

The  $B_d \rightarrow \pi^\mp K^\pm$  amplitudes  $A$  and  $\overline{A}$  can also be combined with those of the charged  $B$ -meson decays  $B^\pm \rightarrow \pi^\pm K$ ,  $\pi^0 K^\pm$ . Neglecting  $P_{\text{ew}}^C$  in the amplitude relation (6), we obtain the triangle relations

$$P + T + A = 0 \quad (89)$$

$$\overline{P} + \overline{T} + \overline{A} = 0. \quad (90)$$

If, moreover, we neglect rescattering effects, we have  $P = \overline{P}$ , and consequently arrive at the two triangles represented by the thick solid lines in Fig. 12. If the angle  $\varphi$  is known from the  $B_s \rightarrow K^+ K^-$  analysis, both  $\gamma$  and  $|T|$  can be simultaneously determined by requiring  $|T| = |\overline{T}|$ . Using the strategies proposed in [6, 7], which make use of  $B^\pm \rightarrow K^\pm K$  decays, rescattering processes can be taken into account in this approach to

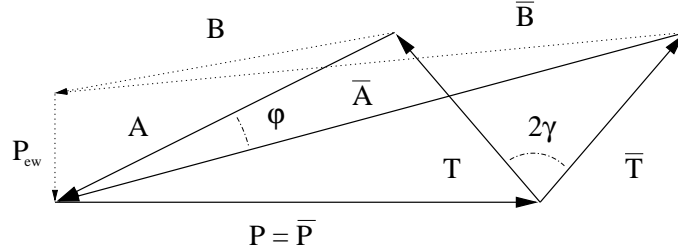


Figure 12: Simple strategy to determine  $\gamma$  with the help of the decays  $B_d \rightarrow \pi^\mp K^\pm$  and  $B^\pm \rightarrow \pi^\pm K$  (thick solid lines), and to obtain insights into electroweak penguins by using in addition  $B^\pm \rightarrow \pi^0 K^\pm$  (thin dotted lines). Here rescattering effects have been neglected and it has been assumed that “colour suppression” is effective.

determine  $\gamma$ . Its theoretical accuracy is limited by  $SU(3)$ -breaking effects and “colour-suppressed” electroweak penguins. Let us note that if  $\varphi$  is unknown,  $|T|$  has to be fixed in order to extract  $\gamma$ . This construction then corresponds to the one proposed in [3]. If rescattering processes play a minor role and the hypothesis of “colour suppression” works in  $B \rightarrow \pi K$  decays, we have  $T + C \approx T$ , and can determine  $|T|$  with the help of (65). Moreover, if we use in addition the amplitudes  $B \equiv \sqrt{2} A(B^+ \rightarrow \pi^0 K^+)$  and  $\bar{B} \equiv \sqrt{2} A(B^- \rightarrow \pi^0 K^-)$ , the electroweak penguin amplitude  $P_{\text{ew}}$  can be determined [3, 36]. To this end, the relation (39) with  $C = 0$  is used:

$$P + T + B + P_{\text{ew}} = 0, \quad (91)$$

as well as its CP conjugate with  $P = \bar{P}$ , which holds for small rescattering effects:

$$P + \bar{T} + \bar{B} + P_{\text{ew}} = 0. \quad (92)$$

This strategy is also illustrated in Fig. 12, where the amplitudes  $B$ ,  $\bar{B}$  and  $P_{\text{ew}}$  are represented by the thin dotted lines.

## 7 Conclusions

In summary, we have performed an analysis of the combinations  $B^\pm \rightarrow \pi^\pm K$ ,  $\pi^0 K^\pm$  and  $B_d \rightarrow \pi^0 K$ ,  $\pi^\mp K^\pm$  of charged and neutral  $B$  decays within a completely general formalism, taking into account both electroweak penguin and rescattering effects. Originally, this formalism was developed in [6] to probe the CKM angle  $\gamma$  with the help of the decays  $B^\pm \rightarrow \pi^\pm K$  and  $B_d \rightarrow \pi^\mp K^\pm$ , but it can also be applied to these combinations of charged and neutral  $B$  decays, if straightforward replacements of variables are performed. In this manner, we could obtain a unified picture of  $B \rightarrow \pi K$  decays, which is useful for the comparison of the various approaches using these modes to probe the CKM angle  $\gamma$ .

Following these lines, we were in a position to generalize the strategies to constrain and determine  $\gamma$  with the help of  $B^\pm \rightarrow \pi^\pm K$ ,  $\pi^0 K^\pm$  decays, which were recently pointed

out by Neubert and Rosner [18, 19]. This allowed us to investigate the sensitivity of these methods to the various assumptions made in [18, 19], in particular to the neglect of rescattering processes of the kind  $B^+ \rightarrow \{\pi^0 K^+\} \rightarrow \pi^+ K^0$ . We have demonstrated that such final-state interaction effects may lead to uncertainties similar to those affecting the  $B^\pm \rightarrow \pi^\pm K$ ,  $B_d \rightarrow \pi^\mp K^\pm$  strategies. It would be indicated experimentally that such processes play in fact an important role, if future experiments should find a sizeable value of the CP asymmetry arising in  $B^\pm \rightarrow \pi^\pm K$ , or a significant enhancement of the  $B^\pm \rightarrow K^\pm K$ ,  $B_d \rightarrow K^+ K^-$  branching ratios with respect to their “short-distance” expectations. In this case, our completely general formalism would allow us to take into account the rescattering effects with the help of the strategies proposed in [6, 7], making use of  $B^\pm \rightarrow K^\pm K$  decays. Unfortunately, it is not possible to control also non-factorizable  $SU(3)$ -breaking effects in a similar manner. Using our general formulae, we found that such effects may have an important impact on the information on the CKM angle  $\gamma$  provided by the  $B^\pm \rightarrow \pi^\pm K$ ,  $\pi^0 K^\pm$  modes.

We have also proposed a new strategy to probe the CKM angle  $\gamma$  with the help of the neutral decays  $B_d \rightarrow \pi^0 K$ ,  $\pi^\mp K^\pm$ , requiring a time-dependent analysis of  $B_d \rightarrow \pi^0 K_S$ . Although this method is more difficult from an experimental point of view, it is theoretically cleaner than the  $B^\pm \rightarrow \pi^\pm K$ ,  $\pi^0 K^\pm$  approach. The point is that final-state interaction effects can be taken into account in a clean way with the help of the direct and mixing-induced CP-violating observables of the decay  $B_d \rightarrow \pi^0 K_S$ . However, the uncertainties related to non-factorizable  $SU(3)$ -breaking corrections are similar to those affecting the  $B^\pm \rightarrow \pi^\pm K$ ,  $\pi^0 K^\pm$  strategy.

In addition to an accurate measurement of all charged and neutral  $B \rightarrow \pi K$  modes, an analysis of the decay  $B_s \rightarrow K^+ K^-$  would be very useful, allowing a variety of ways to combine its observables with those of the  $B \rightarrow \pi K$  decays to probe the CKM angle  $\gamma$  and to obtain insights into electroweak penguins. The former decays can already be studied at the  $e^+e^-$   $B$ -factories (BaBar, BELLE, CLEO III), which will start to operate at the  $\Upsilon(4S)$  resonance in the near future. In fact, the CLEO collaboration has already reported the first results for these modes. On the other hand, dedicated  $B$ -physics experiments at hadron machines appear to be the natural place to explore  $B_s$  decays.

Let us now critically compare the virtues and weaknesses of the various approaches discussed in this paper. The advantage of the  $B^\pm \rightarrow \pi^\pm K$ ,  $\pi^0 K^\pm$  and  $B_d \rightarrow \pi^0 K$ ,  $\pi^\mp K^\pm$  strategies in comparison with the one using the decays  $B^\pm \rightarrow \pi^\pm K$  and  $B_d \rightarrow \pi^\mp K^\pm$  is that the parameters  $r_{(c,n)}$  can be determined with the help of the decay  $B^+ \rightarrow \pi^+ \pi^0$  by using only the  $SU(3)$  flavour symmetry, and that the electroweak penguins can be theoretically controlled by again making use of  $SU(3)$  flavour symmetry arguments. However, a possible weakness of this approach is the fact that non-factorizable  $SU(3)$ -breaking corrections, which may have an important impact, cannot be treated in a quantitative way at present. In the  $B^\pm \rightarrow \pi^\pm K$ ,  $B_d \rightarrow \pi^\mp K^\pm$  strategy, “factorization” or “colour suppression” has to be employed to fix the parameter  $r$ , and it is more difficult to control the electroweak penguins theoretically. Their importance is strongly related to rescattering effects and to the question of “colour suppression” in  $B \rightarrow \pi K$  decays, which can be probed, for instance, through the CP-violating observables of the decay  $B_d \rightarrow \pi^0 K_S$ .

The prospects to probe  $\gamma$  with the help of the decays  $B^\pm \rightarrow \pi^\pm K$  and  $B_d \rightarrow \pi^\mp K^\pm$  are good, even if the present central value of  $R = 1$  should be confirmed by future data. Although the combined branching ratios of these modes would imply no useful constraints on  $\gamma$  in this case, as soon as CP violation in  $B_d \rightarrow \pi^\mp K^\pm$  decays is observed, contours in the  $\gamma$ - $r$  plane can be fixed, allowing the extraction of  $\gamma$ . In our illustrative example, we found contours with the interesting feature that the extracted value of  $\gamma$  is very insensitive to the value of  $r$ . Consequently, in such a fortunate situation, this strategy to determine  $\gamma$  would not be weakened by the fact that the uncertainty of  $r$  may be larger than that of  $r_c$ . On the other hand, in the  $B^\pm \rightarrow \pi^\pm K, \pi^0 K^\pm$  case, our quantitative example gave less promising contours in the  $\gamma$ - $r_c$  plane, where the extracted value of  $\gamma$  shows a sizeable dependence on  $r_c$ . Clearly time will tell which approach is more promising for the future  $B$ -factories.

An accurate measurement of  $B$ -meson decays into  $\pi K$ ,  $\pi\pi$  and  $KK$  final states is an important goal for future dedicated  $B$ -physics experiments. The physics potential of these modes is very rich, allowing several strategies to probe CKM phases and to shed light on the issue of rescattering effects and electroweak penguins. Also certain  $B_s$  decays are very useful in this respect. We are optimistic that the  $B$ -factory era, which is just ahead of us, will lead to many interesting and exciting results.

#### *Acknowledgements*

We would like to thank Gerhard Buchalla for discussions. A.J.B. would like to thank the CERN theory group for its hospitality during his stay at CERN. This work was partly supported by the German Bundesministerium für Bildung und Forschung under contract 06 TM 874 and by the DFG project Li 519/2-2.



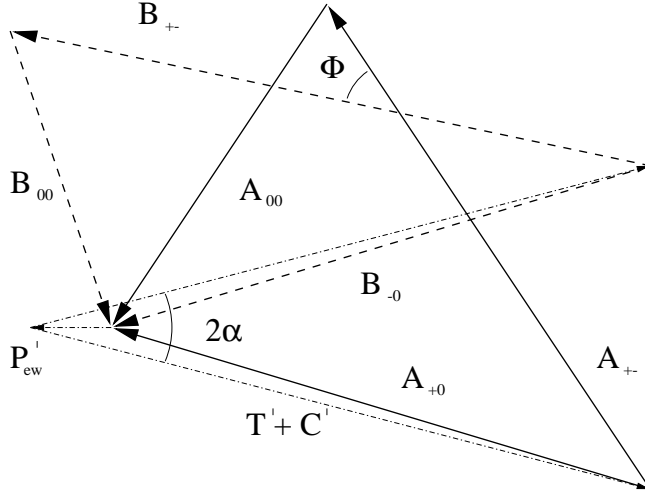


Figure 13: Determination of the CKM angle  $\alpha$  by means of  $B \rightarrow \pi\pi$  isospin relations in the presence of electroweak penguins.

## Appendix: Controlling Electroweak Penguins in the $\alpha$ Determination from $B \rightarrow \pi\pi$ Decays

In this appendix, we point out that a theoretical input similar to (66) allows us to take into account electroweak penguin topologies in the determination of the CKM angle  $\alpha$  with the help of the Gronau–London method [35], using the  $B \rightarrow \pi\pi$  isospin relation

$$A_{+-} + A_{00} = A_{+0} \quad (93)$$

with

$$A_{+-} \equiv A(B_d^0 \rightarrow \pi^+\pi^-), \quad A_{00} \equiv \sqrt{2} A(B_d^0 \rightarrow \pi^0\pi^0), \quad A_{+0} \equiv \sqrt{2} A(B^+ \rightarrow \pi^+\pi^0). \quad (94)$$

We have illustrated this approach in Fig. 13, where

$$B_{+-} \equiv e^{-i2\beta} \bar{A}_{+-}, \quad B_{00} \equiv e^{-i2\beta} \bar{A}_{00}, \quad B_{-0} \equiv e^{-i2\beta} \bar{A}_{+0}, \quad (95)$$

and  $\beta = 180^\circ - \alpha - \gamma$  denotes another angle of the unitarity triangle. The amplitude  $A_{+0}$  can be decomposed as follows:

$$A_{+0} = -[(T' + C') + P'_{\text{ew}}], \quad (96)$$

where the  $\bar{b} \rightarrow \bar{d}$  amplitudes  $T' + C'$  and  $P'_{\text{ew}}$  are defined to be proportional to the CKM factors  $\lambda_u^{(d)}$  and  $\lambda_t^{(d)}$ , respectively. This definition of  $P'_{\text{ew}}$  is useful in the present case, as it gives [17]

$$\overline{P'_{\text{ew}}} = e^{2i\beta} P'_{\text{ew}}. \quad (97)$$

Note that the amplitudes  $(T + C)_{\bar{b} \rightarrow \bar{d}}$  and  $(P_{\text{ew}})_{\bar{b} \rightarrow \bar{d}}$  in (66) are defined to be proportional to  $\lambda_u^{(d)}$  and  $\lambda_c^{(d)}$ , respectively, which is the appropriate definition for the strategies to probe the CKM angle  $\gamma$  discussed in this paper. Proceeding as in Subsection 2.2 and using a similar theoretical input, we obtain (see also [3])

$$\left( \frac{P'_{\text{ew}}}{T' + C'} \right)_{\bar{b} \rightarrow \bar{d}} = \frac{3}{2} \left[ \frac{C_9(\mu) + C_{10}(\mu)}{C_1(\mu) + C_2(\mu)} \right] \frac{|V_{td}|}{|V_{ub}|} e^{i\alpha} = -1.3 \times 10^{-2} \times \frac{|V_{td}|}{|V_{ub}|} e^{i\alpha}. \quad (98)$$

In contrast to (48), the  $SU(2)$  isospin symmetry suffices to derive this expression, i.e. no  $SU(3)$  flavour symmetry arguments have to be used to this end.

With all this information at hand, the determination of  $\alpha$  from  $B \rightarrow \pi\pi$  decays in the presence of electroweak penguins can be accomplished as follows:

1. The two triangles represented by the thick solid and dashed lines can be determined by measuring all  $B, \bar{B} \rightarrow \pi\pi$  branching ratios, while their relative orientation, i.e. the angle  $\Phi$ , can be fixed by measuring mixing-induced CP violation in the mode  $B_d \rightarrow \pi^+\pi^-$  (a detailed discussion can be found in [17]).
2. The two squashed triangles in Fig. 13 represent the relation (96) and its CP conjugate, multiplied by  $e^{-i2\beta}$ . The inspection of these triangles, together with the phase in (98), tells us that  $P'_{\text{ew}}$  lies on the line that bisects the angle between the amplitudes  $A_{+0}$  and  $B_{-0}$ .
3. Since (98) implies  $|P'_{\text{ew}}| \ll |T' + C'|$ , we have, to a very good approximation:

$$|P'_{\text{ew}}| = 1.3 \times 10^{-2} \times \frac{|V_{td}|}{|V_{ub}|} |A_{+0}|, \quad (99)$$

where  $|A_{+0}|$  is obtained from  $\text{BR}(B^+ \rightarrow \pi^+\pi^0)$ . Equation (99), in combination with the minus sign in (98) and the two previous steps, allows us to complete the construction shown in Fig. 13, and to determine the CKM angle  $\alpha$ .

## References

- [1] CLEO Collaboration (R. Godang et al.), *Phys. Rev. Lett.* **80** (1998) 3456.
- [2] For a review, see R. Fleischer, preprint CERN-TH/98-296 (1998) [hep-ph/9809302], invited talk given at the 29th International Conference on High Energy Physics (ICHEP '98), Vancouver, Canada, 23–29 July 1998; to appear in the proceedings.
- [3] R. Fleischer, *Phys. Lett.* **B365** (1996) 399.
- [4] M. Gronau and J.L. Rosner, *Phys. Rev.* **D57** (1998) 6843.
- [5] R. Fleischer and T. Mannel, *Phys. Rev.* **D57** (1998) 2752.

- [6] R. Fleischer, *Eur. Phys. J. C* (1998) DOI 10.1007/s100529800919 [hep-ph/9802433].
- [7] R. Fleischer, *Phys. Lett.* **B435** (1998) 221.
- [8] CLEO Collaboration (M. Artuso et al.), preprint CLEO CONF 98-20; J. Alexander, plenary talk given at the 29th International Conference on High Energy Physics (ICHEP '98), Vancouver, Canada, 23–29 July 1998; to appear in the proceedings.
- [9] Y. Grossman, Y. Nir, S. Plaszczynski and M.-H. Schune, *Nucl. Phys.* **B511** (1998) 69.
- [10] M. Gronau, J.L. Rosner and D. London, *Phys. Rev. Lett.* **73** (1994) 21.
- [11] O.F. Hernández, D. London, M. Gronau and J.L. Rosner, *Phys. Lett.* **B333** (1994) 500; *Phys. Rev.* **D50** (1994) 4529.
- [12] N.G. Deshpande and X.-G. He, *Phys. Rev. Lett.* **74** (1995) 26 [E: **74** (1995) 4099].
- [13] R. Fleischer, *Z. Phys.* **C62** (1994) 81; *Phys. Lett.* **B321** (1994) 259.
- [14] R. Fleischer, *Phys. Lett.* **B332** (1994) 419.
- [15] For a recent study, see A. Ali, G. Kramer and C.-D. Lü, *Phys. Rev.* **D58** (1998) 094009.
- [16] M. Neubert, *Phys. Lett.* **B424** (1998) 152.
- [17] A.J. Buras and R. Fleischer, *Phys. Lett.* **B365** (1996) 390.
- [18] M. Neubert and J.L. Rosner, preprint CERN-TH/98-273 (1998) [hep-ph/9808493].
- [19] M. Neubert and J.L. Rosner, preprint CERN-TH/98-293 (1998) [hep-ph/9809311].
- [20] L. Wolfenstein, *Phys. Rev.* **D52** (1995) 537; J. Donoghue, E. Golowich, A. Petrov and J. Soares, *Phys. Rev. Lett.* **77** (1996) 2178; B. Blok and I. Halperin, *Phys. Lett.* **B385** (1996) 324; B. Blok, M. Gronau and J.L. Rosner, *Phys. Rev. Lett.* **78** (1997) 3999.
- [21] J.-M. Gérard and J. Weyers, preprint UCL-IPT-97-18 (1997) [hep-ph/9711469].
- [22] A.F. Falk, A.L. Kagan, Y. Nir and A.A. Petrov, *Phys. Rev.* **D57** (1998) 4290.
- [23] D. Atwood and A. Soni, *Phys. Rev.* **D58** (1998) 036005.
- [24] M. Gronau and J.L. Rosner, preprint EFI-98-23 (1998) [hep-ph/9806348].
- [25] A.J. Buras, R. Fleischer and T. Mannel, preprint CERN-TH/97-307 (1997) [hep-ph/9711262], to appear in *Nucl. Phys.* **B**.
- [26] L. Wolfenstein, *Phys. Rev. Lett.* **51** (1983) 1945.

- [27] A.J. Buras, M.E. Lautenbacher and G. Ostermaier, *Phys. Rev.* **D50** (1994) 3433.
- [28] P. Rosnet, talk given at the 29th International Conference on High Energy Physics (ICHEP '98), Vancouver, Canada, 23–29 July 1998; to appear in the proceedings.
- [29] G. Buchalla, A.J. Buras and M.E. Lautenbacher, *Rev. Mod. Phys.* **68** (1996) 1125.
- [30] Y. Nir and H.R. Quinn, *Phys. Rev. Lett.* **67** (1991) 541.
- [31] M. Gronau, O.F. Hernández, D. London and J.L. Rosner, *Phys. Rev.* **D52** (1995) 6374.
- [32] M. Gronau and J.L. Rosner, preprint SLAC-PUB-7945 (1998) [hep-ph/9809384].
- [33] F. Würthwein and P. Gaidarev, preprint CALT-68-2153 (1997) [hep-ph/9712531].
- [34] This range corresponds to an update of the analysis performed in: A.J. Buras, preprint TUM-HEP-316-98 (1998) [hep-ph/9806471]; to appear in *Probing the Standard Model of Particle Interactions*, eds. F. David and R. Gupta (Elsevier Science B.V., Amsterdam, 1998).
- [35] M. Gronau and D. London, *Phys. Rev. Lett.* **65** (1990) 3381.
- [36] R. Fleischer, *Int. J. Mod. Phys.* **A12** (1997) 2459.
- [37] A.B. Carter and A.I. Sanda, *Phys. Rev. Lett.* **45** (1980) 952; *Phys. Rev.* **D23** (1981) 1567; I.I. Bigi and A.I. Sanda, *Nucl. Phys.* **B193** (1981) 85.
- [38] A.J. Buras and R. Fleischer, *Phys. Lett.* **B360** (1995) 138.
- [39] R. Fleischer, *Phys. Rev.* **D58** (1998) 093001.
- [40] R. Fleischer and I. Dunietz, *Phys. Rev.* **D55** (1997) 259.
- [41] C.S. Kim, D. London and T. Yoshikawa, *Phys. Rev.* **D57** (1998) 4010.
- [42] For a recent calculation of  $\Delta\Gamma_s$ , see M. Beneke, G. Buchalla, C. Greub, A. Lenz and U. Nierste, preprint CERN-TH/98-261 (1998) [hep-ph/9808385].
- [43] I. Dunietz, *Phys. Rev.* **D52** (1995) 3048.
- [44] A.S. Dighe, I. Dunietz and R. Fleischer, [hep-ph/9804253], *Eur. Phys. J. C* (1998) DOI 10.1007/s100529800954.
- [45] M. Gronau, O.F. Hernández, D. London and J.L. Rosner, *Phys. Rev.* **D52** (1995) 6356.
- [46] R. Aleksan, I. Dunietz and B. Kayser, *Z. Phys.* **C54** (1992) 653.